Geospatial Inequality in the Green Transition: Pollution Redistribution from Electric Vehicles*

Jianwei Ai† *Cornell*
Zheng Xiao‡ *DUFE*
Wendong Zhang§ *Cornell*

May 30, 2026

Abstract

Electric vehicles (EVs) are widely recognized to deliver environmental benefits by replacing tailpipe emissions with electricity. This paper shows that when electricity generation remains coal-intensive, EV adoption reduces urban air pollution but also redistributes it across space. Using monthly city-level comprehensive vehicle registration data and satellite-based pollution measures around power plants in China, we find that EV adoption *reduces* urban pollution while *increasing* pollution exposure near coal-fired power plants. The results are robust to extensive controls and instrumental-variable estimates based on charging-station expansion. We further use a new method that incorporates inter-regional electricity transmission, addressing a major challenge in identifying the causal environmental impacts of electrification. Pollution displacement generates both *intra-city* and *inter-city* environmental inequality, with roughly *two-thirds* arising across cities and *one-third* within cities, highlighting the importance of power-sector decarbonization in evaluating the environmental justice implications of EV adoption.

Keywords: Electric Vehicle; Air Pollution; Power Plant; Environmental Justice
JEL Classification: Q52; Q53; R23; L94.

*We thank participants at various seminars and conferences for helpful comments. We also thank Chao Han for sharing some of the data used in this research and generous discussion on policies. All errors are our own.

†Charles H. Dyson School of Applied Economics and Management, SC Johnson College of Business, Cornell University. E-mail: jianwei.ai@cornell.edu.

‡Center for Industrial and Business Organization, Dongbei University of Finance and Economics. E-mail: zhengxiao5170@126.com.

§Charles H. Dyson School of Applied Economics and Management, SC Johnson College of Business, Cornell University. E-mail: wendongz@cornell.edu.

1 Introduction

The electrification of the transportation sector is widely championed as a critical pathway for decarbonization and urban air quality improvement. Global efforts to decarbonize transportation have sparked an unprecedented shift toward electric vehicles (EVs) (Barwick et al., 2024; Fang et al., 2025; Gillingham et al., 2025). Nowhere is this transition more rapid than in China, which has emerged as the world's largest market for EVs, accounting for over half of global EV sales in recent years.[1] This shift is widely viewed as a cornerstone of climate policy, based on the premise that electrifying transportation will reduce local air pollution and global carbon emissions. The implicit assumption behind this view is that the environmental benefits of EVs accrue broadly and equitably. However, while the *tailpipe* is clean, the *smokestack* powering it may not be. In an economy where coal still accounts for a significant portion of electricity in the long term, the rapid adoption of EVs implies a substantial positive shock to electricity demand, raising a critical yet under-explored question: who gains, and who loses, from the green transition?

The conventional narrative holds that EVs are universally clean because they eliminate tailpipe emissions. However, this perspective overlooks the fact that EVs rely on electricity, and electricity generation remains heavily carbon-intensive in many countries. EV adoption has been spatially uneven and concentrated in more advantaged neighborhoods (Jacqz and Johnston, 2024). When the marginal unit of electricity is generated by fossil fuel power plants, as is common in regions with coal-based grids, electrification does not necessarily eliminate pollution; instead, it shifts it from the point of consumption to the point of electricity production. While the engineering literature has long recognized this possibility, no empirical work has quantified how EV adoption redistributes pollution spatially across the economy (Sioshansi and Denholm, 2010; Michalek et al., 2011; Holland et al., 2016; Hanig et al., 2025). In particular, we lack evidence on whether EV-induced emissions arise primarily near urban consumers, near power plants, or in downwind communities. As a result, policymakers have little guidance on how the environmental benefits of EVs are shared and whether the costs fall disproportionately on vulnerable populations, which definitely raises environmental justice concerns.

This paper provides the first large-scale evidence that EV adoption redistributes air pollution in ways that create both intra-city and inter-city environmental inequality. Using high-resolution satellite measures of multiple air pollutants matched to the universe of power plants in China, we show that EV adoption reduces ambient pollution in adopting cities but

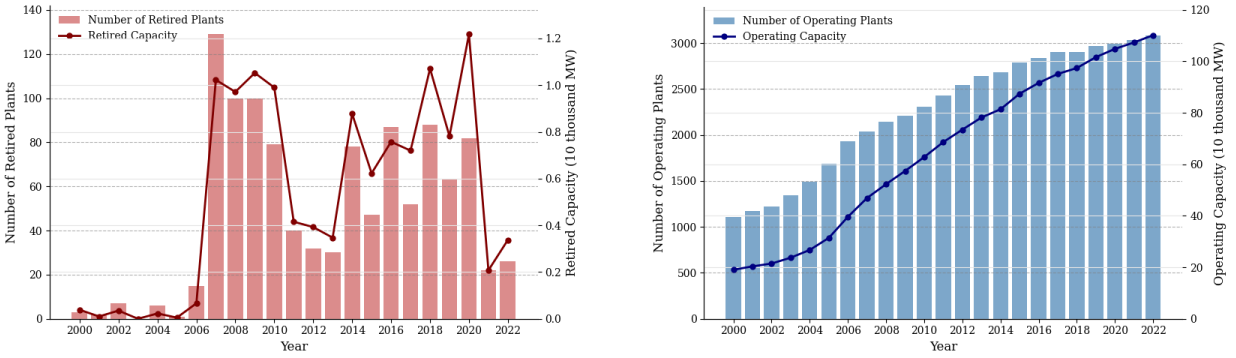
[1] In 2024, China accounted for 80 percent of global EV sales, and major metropolitan areas such as Beijing, Shanghai, and Shenzhen have become showcases of "clean mobility" (The Economic Times, 2024).

increases pollution in communities located near coal-fired power plants in cities that supply the marginal electricity. These effects are economically meaningful, spatially concentrated, and robust across a wide range of empirical strategies. The results demonstrate that when electricity grids remain carbon-intensive, EV adoption produces environmental winners and losers: urban residents benefit from cleaner air, while plant-adjacent and downwind communities, often poorer and less politically influential, bear the cost of higher emissions. Our paper highlights a gap in the clean transition literature, which has largely focused on pollution haven effects driven by the relocation of production in response to regulation, rather than on demand-induced upstream emissions that arise at the point of electricity generation, as in our setting.

China provides an unusually informative setting to identify this mechanism. First, China has the world's largest EV market, accounting for more than half of global EV sales, driven by city-specific adoption policies that generate substantial cross-sectional variation in EV penetration (Fang et al., 2025). Second, China remains heavily reliant on coal-fired power plants, which generate approximately 60 percent of its electricity (Qin and Shearer, 2025).[2] Despite recent policy efforts to reduce coal dependency, the retirement of existing plants has been limited. Figure 1 shows that although the annual number of retired coal-fired power plants has increased rapidly in recent years, the number and operating capacity of existing coal power plants still account for a large share of total electricity generation. These plants are spatially fixed and vary widely in their proximity to population centers, allowing us to detect localized changes in emissions. Third, China's electricity system is characterized by *inter-provincial* transmission and spatial frictions, enabling us to distinguish between local EV-driven load and regional spillovers. Fourth, the availability of satellite pollution measures at a high resolution, combined with monthly plant-level electricity and meteorological data, permits a granular analysis of pollution responses across space. This combination of rapid EV diffusion, coal-dependent electricity supply, fine-grained pollution data, and institutional rigidity provides a unique setting to study how electrification reshapes the distribution of air pollution.

Our empirical analysis proceeds in three steps. First, we estimate the effect of EV penetration on city-level pollution. Consistent with prior work, we find that higher EV adoption significantly reduces average NO_2 concentrations in urban areas, with especially strong effects in cities with high road density. Second, we examine pollution near coal-fired power plants and find the opposite pattern: EV adoption increases NO_2 concentrations within 10 km of power plants by 0.3-0.4 units, with the effects attenuating sharply at 20 km and beyond

[2]We present China's monthly power generation mix from 2016 to 2025 in Figure A.1, illustrating the continued dominance of coal-fired power generation in China.



(a) Number of Retired Plants and Capacity (b) Number of Operating Plants and Capacity

Figure 1: Coal Power Plant Trends in China (2000-2022)

Notes: The left panel (a) shows the annual number of retired coal power plants (left axis) and the total operating capacity (right axis). The right panel (b) shows the total number of operating plants (left axis) and the same operating capacity trend. Capacity is measured in 10,000 MW. Data source: Global Energy Monitor's Global Coal Plant Tracker.

50 km. Strikingly, these increases are concentrated strictly in the downwind direction, consistent with atmospheric transport rather than behavioral or economic confounders. Third, we combine these results to illustrate the full redistribution of pollution from city centers to power plant-adjacent and downwind communities. In settings where electricity generation is spatially distant from urban consumers, EV adoption therefore creates inter-city inequality: the residents who adopt EVs and enjoy cleaner air are not the same individuals who bear the burden of the resulting power-plant emissions. Our results indicate that approximately two-thirds of the resulting environmental inequality comes from inter-cities, while the remaining one-third arises intra-cities.

To address endogeneity concerns, we employ several strategies. First, we introduce province-year fixed effects to absorb policy shocks and energy transitions that vary over time. Second, we control for local economic conditions, EV-related policies, and COVID-19 impacts to rule out the possibility that cities with faster EV adoption simultaneously invest more in pollution abatement or implement other contemporaneous policies. Third, we instrument for EV penetration using the expansion of public charging-station infrastructure, which is driven by provincial and national planning targets and strongly predicts EV uptake but is orthogonal to short-run changes in power-plant emissions. In addition, we use an exposure-share robustness test that constructs EV penetration at the province level, excluding the plant's own city, following the approach of Arkolakis and Walsh (2023) to further separate local adoption from grid-wide electricity demand. Across all of these approaches, the results remain robust and economically significant.

We then explore the possible competing mechanisms, test for alternative explanations, and address specification concerns. First, we estimate a saturated model with controls for economic conditions, such as GDP per capita, industrial development, and population, to address concerns that the observed relationship between EV adoption and pollution redistribution may be confounded by economic development and population dynamics. To further isolate the EV effect, we also examine the relationship in subsamples of regions that experienced stagnant industrial economic growth yet saw increases in EV adoption, ruling out broader economic or demographic shifts as competing mechanisms. Second, we show that hybrid-vehicle adoption and fuel-vehicle adoption do not increase plant-level pollution, ruling out *any vehicle adoption* as a confounding mechanism. Third, we conduct placebo tests using other electricity-generating facilities, such as hydropower, wind, and solar power plants, and find no relationship between EV adoption and pollution at these sites. Fourth, we show that other pollutants, SO_2 and O_3, respond qualitatively similarly, although NO_2 displays the clearest spatial gradient.[3] Finally, we confirm that the results are robust to log transformations, long-difference specifications, and alternative clustering levels. Thus, these analyses strongly support a causal interpretation: EV-induced electricity demand increases emissions at coal power plants, and these emissions impose localized environmental costs.

Finally, we draw implications for policy design and present a back-of-the-envelope cost-benefit analysis. We show that regions relying more heavily on clean electricity do not experience pollution displacement, highlighting the importance of aligning EV adoption with rapid grid decarbonization to avoid widening geospatial inequalities. Focusing on the reduction in very low birth weight due to less air pollution alone, we estimate annual welfare gains of approximately \$3.04 billion, cumulating to \$12.17 billion over 2019-2022. However, pollution displacement to communities near coal-fired power plants imposes an estimated annual cost of \$0.22 billion on disadvantaged communities. While aggregate benefits substantially exceed these localized costs, our results underscore that credible welfare assessments must account for both efficiency gains and distributional equity to ensure an equitable green transition.

The implications extend beyond China. The winners and losers of air pollution reduction across counties are closely related to concerns about environmental justice (Ma, 2020). In any setting where electrification outpaces the decarbonization of the grid, including parts of

[3]We focus on NO_2 because it is the most sensitive and spatially resolved indicator of short-run changes in fossil-fuel combustion from power plants (Liu et al., 2020*b*). First, NO_x emissions respond almost instantaneously to shifts in coal-fired electricity generation, making NO_2 an ideal pollutant for detecting marginal variation induced by EV charging demand. Second, NO_2 is less affected by long-range transport and complex atmospheric chemistry relative to O_3, and exhibits clearer downwind concentration patterns than SO_2, especially in short time windows. These properties make NO_2 the preferred pollutant for identifying spatial redistribution of emissions in response to EV adoption, consistent with prior work linking electricity demand shocks to NO_2 exposures.

the United States, India, and Europe, similar redistribution dynamics are likely to arise.[4] As countries (or regions) pursue aggressive EV targets, recognizing the unequal distribution of environmental costs is crucial for designing equitable climate policy. Our findings suggest that policies accelerating EV adoption should be accompanied by parallel investments in clean electricity generation and targeted protections for communities located near power plants. Without such considerations, the green transition risks reproducing old patterns of environmental inequality under the guise of new technology.

Related Literature. Our paper is related to several strands of literature. First, our paper relates to work on the environmental consequences of EVs and the importance of the electricity generation mix. A growing body of research emphasizes that the environmental benefits of EVs depend critically on the marginal emissions of electricity production (Nehiba, 2024). Holland et al. (2016) show that EV adoption in the United States can reduce local air pollution. Building on these documented environmental gains, a related literature evaluates a variety of policies designed to promote EV adoption, including purchase subsidies (Barwick et al., 2022; Xing et al., 2021), charging infrastructure design and spatial distribution(Li et al., 2017; Li, 2019; Arkolakis et al., 2025), and gasoline vehicle bans (Holland et al., 2021). The rise of EV-related subsidies and industrial policy reflects what Meckling (2025) describes as the *geoeconomic turn* in decarbonization, in which states prioritize strategic control of clean-energy supply chains. Graff Zivin et al. (2014) document substantial spatial and temporal variation in marginal emissions, implying that additional electricity demand, such as that induced by EV charging, can lead to net increases in criteria pollutants in coal-dependent regions.

Engineering and lifecycle analyses reach similar conclusions, showing that EVs may increase NO_x and SO_2 emissions where coal-fired electricity is the marginal electricity source (Michalek et al., 2011; Archsmith et al., 2015). Lin and Wu (2021) further show that when coal dominates the generation mix, electric vehicles can raise carbon emissions. Holland et al. (2019) provided the seminal theoretical framework and simulation evidence suggesting that EVs could redistribute pollution from demand centers to power generation regions. However, empirical evidence verifying this spatial leakage using observed pollution outcomes remains limited, especially in developing economies where the grid is carbon-intensive. We contribute causal evidence that EV adoption reallocates pollution from urban consumers

[4] Hanig et al. (2025) document similar environmental justice patterns associated with EV adoption in the United States. One important distinction, however, is that electricity supply in the U.S. is organized largely through regional grids (e.g., ERCOT in Texas), with limited long-distance transmission across regions (Arkolakis and Walsh, 2023). As a result, pollution displacement effects in the U.S. are predominantly regional rather than national in scope.

to communities near coal-fired power plants, using satellite-based pollution measures from China.

Second, this paper builds on the literature documenting that pollution can shift spatially in response to regulation or changes in production activity. The pollution haven hypothesis posits that economic activity in developed regions often shifts pollution-intensive industries to less developed areas with weaker environmental enforcement (Copeland and Taylor, 2004; Carril-Caccia and Baleix, 2024). Currie et al. (2015) show that U.S. emissions regulations induced *"pollution leakage"* to unregulated plants. Jia et al. (2025) also document evidence of intra-firm pollution leakage, showing that firms strategically shift emissions-intensive production stages across their subsidiaries to exploit regional regulatory disparities. Fowlie et al. (2016) demonstrate that market-based emissions regulation leads firms to reallocate production across space. Shapiro and Walker (2018) similarly show that U.S. environmental regulation reduced domestic pollution but increased pollution embodied in imported goods. We contribute to this literature by showing that pollution displacement can occur not only through firm relocation or production shifting, but also through the adoption of a consumer clean technology like electric vehicles, and mediated through existing infrastructure, when the underlying power system remains fossil-fuel intensive.

Third, our paper contributes to research on environmental inequality and environmental justice. Extensive literature documents that pollution burdens are not uniformly shared across populations and places, driven by residential sorting, historical industrial siting, and broader distributional forces (Banzhaf et al., 2019; Currie et al., 2023; Colmer et al., 2024; Mei et al., 2025). Moreover, downwind communities disproportionately bear the externalities of fossil fuel electricity generation (Davis, 2011; Holladay and LaRiviere, 2017), while recent literature emphasizes that both emissions and policy incidence are inherently spatial (Domínguez-Iino, 2023; Balboni and Shapiro, 2025). Within the transportation sector, spatial inequality has intensified as road freight drives intercity emissions disparities (Yu et al., 2026). Although market-based climate policies can sometimes mitigate environmental justice gaps (Hernandez-Cortes and Meng, 2023), we identify a new mechanism of inequality arising from clean technology adoption. While EV subsidies are regressive in consumption incidence because they benefit higher-income urban households (Borenstein and Davis, 2016; Muehlegger and Rapson, 2022), we show they are also regressive in pollution incidence. By tracing the spatial displacement of emissions from EV charging, we document a reallocation of exposure from urban centers to lower-income power plant communities. This process generates both intracity and intercity disparities. Our findings contribute to the growing environmental justice literature in China and demonstrate how the green transition may reshape rather than eliminate environmental inequality.

Finally, this paper relates to broader work on energy transitions and the distributional consequences of climate policy. Recent research emphasizes that the benefits and burdens of decarbonization depend on the spatial distribution of energy infrastructure (García-Muros et al., 2022; Pizer and Sexton, 2019) and the pace of grid decarbonization relative to electrification. Fowlie et al. (2020) argue that climate policies must explicitly consider local environmental justice implications to avoid creating winners and losers along spatial and socioeconomic dimensions. Schöngart et al. (2025) document that high-income groups disproportionately contribute to climate extremes worldwide, underscoring the importance of distributional analysis in environmental policy. We show that when electrification outpaces decarbonization, EV adoption can create unintended distributional consequences and even regressive environmental outcomes. Our findings, therefore, highlight the need to evaluate clean technology policies not only through their aggregate emissions impact, but also through their spatial and distributional consequences.

The remainder of the paper is organized as follows. Section 2 provides institutional and technological background on EV adoption and electricity generation in China. Section 3 presents a conceptual framework that clarifies how electrification can redistribute pollution across space. Section 4 describes the construction of the satellite-based pollution dataset, EV adoption measures, and plant-level characteristics. Section 5 outlines the empirical design. Section 6 reports the baseline results on the effects of EV adoption on pollution near power plants, while Section 7 presents a series of robustness and placebo tests. Section 8 explores mechanisms, distributional implications, policy implications, and the back-of-the-envelope cost-benefit analysis. Section 9 concludes.

2 Background

2.1 Electric Vehicle Market Share

Over the past decade, China has established itself as the world's largest market for new energy vehicles (NEVs), as shown in Figure 2 (Xing et al., 2021; Li et al., 2022; Fang et al., 2025).[5] This rapid electrification has been driven by a *"carrot and stick"* policy framework designed to reduce urban air pollution and foster industrial leadership simultaneously. On the supply side, the central government initiated generous purchase subsidies in 2009, which at their peak covered up to 60,000 RMB (approximately $8,500) per vehicle (Liu et al.,

[5]Our analysis focuses on the period from 2019 to 2022 for two main reasons. First, EV penetration increased rapidly during this period. Second, satellite-based pollution data exhibit substantially higher quality beginning around November 2018. We additionally use ground-based monitoring station data as a robustness check to provide complementary evidence.

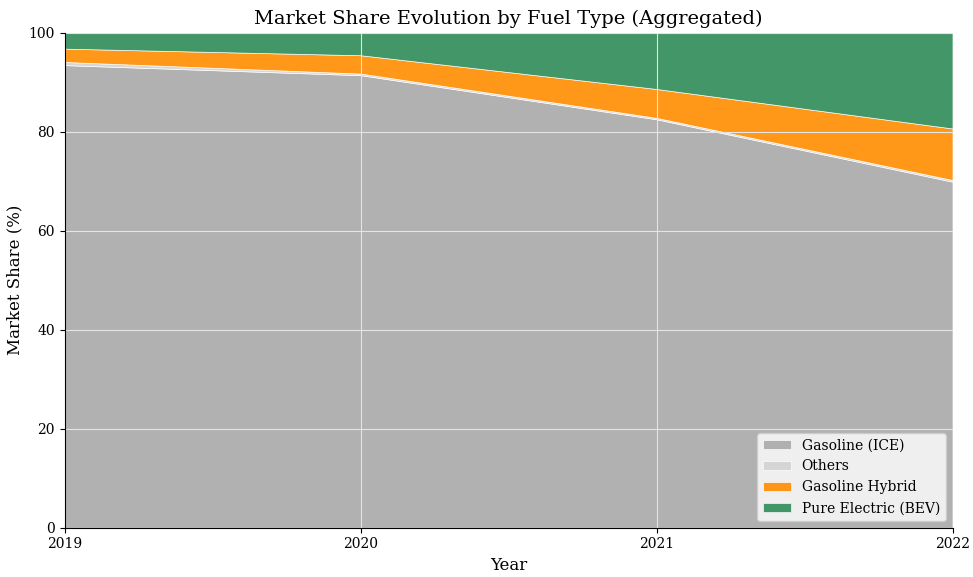


Figure 2: Market Share Evolution by Fuel Type from 2019 to 2022

Notes: This figure illustrates the changing composition of the Chinese passenger vehicle market from 2019 to 2022. The chart is constructed as a 100% stacked area plot, where the vertical axis represents the percentage share of total annual sales. The categories are aggregated as follows: *"Gasoline (ICE)"* (grey area) represents traditional internal combustion engine vehicles; *"Gasoline Hybrid"* (orange area) includes non-plug-in hybrids; *"Pure Electric (BEV)"* (green area) represents battery electric vehicles; and *"Others"* (light grey area) includes diesel, natural gas, fuel cell, and methanol vehicles.

2020*a*). While these national subsidies have gradually tapered since 2017 to encourage market consolidation, they were complemented by distinct local incentives.

On the demand side, the most potent policy tools have been non-monetary restrictions on internal combustion engine vehicles (ICEVs). Major metropolises such as Beijing, Shanghai, and Shenzhen adhere to strict license plate quota systems to combat congestion.[6] In contrast, NEVs are frequently exempt from these quotas, granted *"green license plates"* directly, and exempted from day-of-week driving bans (Barwick et al., 2022; Li et al., 2022). This regulatory asymmetry has concentrated EV adoption in affluent, highly congested coastal cities, creating a sharp spatial divergence in the geography of the vehicle fleet (Fang et al., 2025).

[6]In these cities, obtaining a license plate for a conventional gasoline car often requires participating in a monthly lottery with winning probabilities as low as 0.2% or paying auction fees exceeding $14,000 (Zhuge et al., 2020; Xing et al., 2021).

2.2 The Coal-Dominated Power Sector

Despite leading the world in renewable energy installation, China's electrical grid remains heavily dependent on coal. Also, Coal-fired power plants remain major sources of NO_2 and SO_2 in China, and the distributional effects of their phasedown have been shown to be uneven across communities (Li et al., 2025). Understanding whether EV adoption amplifies or mitigates these spatial inequalities is essential. As of 2023, thermal power still accounted for nearly 60% of total electricity generation (China Energy Transformation Programme, 2025). The sector has undergone significant structural adjustments under the *"War on Pollution"* announced in 2013 (Greenstone et al., 2021). The central government has aggressively retired small, inefficient, and highly polluting generation units, typically those under 300 MW, while simultaneously sanctioning the construction of massive ultra-supercritical coal bases (Harvey, 2024).

This consolidation strategy has implications for emission intensity. While modern plants are equipped with flue-gas desulfurization and selective catalytic reduction systems, the absolute volume of coal combustion has continued to rise (Zhang et al., 2022). The clean energy transition in the power sector has thus far been characterized by a substitution of capital for efficiency rather than a complete departure from fossil fuels. Consequently, the marginal kilowatt-hour (kWh) demanded by an EV charging at night when solar generation is offline is overwhelmingly likely to be supplied by a coal-fired unit (Simshauser and Wild, 2025). In a coal-dominated grid, EV adoption may therefore reduce urban air pollution while simultaneously increasing pollution exposure in downwind, rural, or disadvantaged communities located near power plants, precisely the distributional mechanism this paper examines.

2.3 Spatial Mismatch and Power Transmission

A defining feature of China's energy geography is the pronounced spatial mismatch between electricity supply and demand. Most coal reserves and thermal generation capacity are concentrated in the resource-rich northern and western provinces, such as Inner Mongolia, Shanxi, and Xinjiang, while electricity consumption is heavily concentrated in the industrialized and densely populated eastern and southern coastal regions (Jia et al., 2023). This geographic disparity has long shaped China's energy policy and plays a central role in determining the environmental consequences of EV adoption.

To reconcile this imbalance, China has developed the world's most extensive network of Ultra-High Voltage (UHV) transmission lines as part of the *West-to-East Power Transmission* initiative (Gao and Zhao, 2025). These long-distance corridors enable coastal demand

centers to import vast quantities of baseload electricity from inland coal-producing provinces (Wang et al., 2023; Ren et al., 2026). In the context of our study, the UHV network serves as the physical conduit through which EV-induced electricity demand in coastal cities is met by distant coal-fired generation.

This structure generates a spatial decoupling between where electricity is consumed and where pollution is produced. An EV plugged in Shanghai, for example, is disproportionately likely to draw marginal electricity generated more than 1,000 kilometers away in Inner Mongolia. As a result, EV adoption removes tailpipe emissions from high-density urban areas but increases smokestack emissions in the remote and often disadvantaged regions that host power plants. This long-range redistribution mechanism is fundamental to assessing the environmental justice implications of China's green transition across cities.

3 Conceptual Framework

EV adoption affects air pollution through two distinct channels: (i) eliminating tailpipe emissions in urban areas, and (ii) increasing electricity demand that is met by coal-fired power plants. Because these plants are spatially distant from most urban centers and their emissions disperse downwind, the environmental consequences of EVs depend critically on where pollution is produced, where it is transported, and who is exposed.

We use a simple model to clarify how EV adoption can generate both environmental benefits and environmental inequality. Households in cities gain from replacing gasoline vehicles with EVs, which reduces local tailpipe emissions and provides direct consumption benefits. However, EVs increase electricity demand, and in coal-dependent power systems, this induces additional generation at nearby power plants (Hanig et al., 2025). Because plant emissions predominantly affect the downwind and surrounding communities rather than the urban adopters, the upstream pollution burden rises even as urban air quality improves. When the private and local environmental benefits of EVs in the adopting city exceed the small share of plant emissions that drift back to the same city, city residents experience a welfare gain, while plant-adjacent communities unambiguously lose. In a multi-city grid where electricity flows across jurisdictions, EV adoption in one city can also raise pollution in other regions that host generation capacity. The model therefore predicts, and the data confirm, that EV adoption in carbon-intensive grids creates both intra-city and inter-city environmental inequality through spatial pollution redistribution.

This framework yields two testable predictions. First, citywide air quality should improve as EV penetration increases due to the removal of tailpipe emissions. Second, pollution should rise in plant-adjacent and downwind communities, with magnitudes that attenuate

with distance from the power plant and correspond to prevailing wind patterns. In settings with inter-city electricity transmission, EV adoption in one city may also raise pollution in other cities that share the same electricity-generating assets. To improve readability, we leave the formal analysis in the Appendix D.

4 Data

4.1 Vehicle Sales and EV Charging Stations Data

We compile monthly data on vehicle sales and registrations at the city level from 2019 to 2022. This data is sourced from official vehicle registration records maintained under the *Compulsory Traffic Accident Liability Insurance* system, which provides near-universal coverage of newly registered vehicles in China.[7] The dataset includes pure electric vehicles, battery electric vehicles (BEVs), and plug-in hybrid electric vehicles (PHEVs), allowing us to track the diffusion of new energy vehicles across cities comprehensively.

A key empirical challenge in studying the effects of EV adoption is that adoption may be correlated with unobserved local characteristics, such as environmental preferences or income growth. To address this, we collect a dataset documenting the rollout of EV charging station infrastructure, specifically public charging piles and fast-charging stations, introduced at different times and intensities across cities. Because national policy required local governments to meet charging infrastructure targets but allowed substantial discretion in timing and build-out, this process generates sharp cross-sectional and intertemporal variation in EV adoption. We use this staggered introduction as a source of plausibly exogenous variation in EV adoption.

Table 1 summarizes the national pattern of vehicle registrations by fuel type between 2019 and 2022. While sales of conventional gasoline vehicles declined steadily over the period, sales of BEVs and gasoline hybrids increased dramatically. BEVs in particular expanded from roughly 669,675 units in 2019 to nearly 4 million in 2022, showing both rapid technological advancement and supportive policy incentives. Overall, our dataset captures approximately 74.5% of the national *new energy vehicle* market, giving us a reliable foundation to analyze the environmental and distributional consequences of EV adoption.

[7]This data source records the number of vehicles for which compulsory traffic liability insurance is purchased after sales completion. Because this insurance is legally required for vehicle registration and on-road operation, insurance registration data closely track actual vehicle deliveries to end consumers and provide a reliable measure of realized final demand.

Table 1: Vehicle Sales by Fuel Type

Fuel Type	2019	2020	2021	2022	Total
Gasoline	19,244,375	17,511,942	16,870,417	13,844,288	67,471,024
Diesel	22,314	11,910	16,505	14,240	64,969
Natural Gas	4,030	17,211	20,017	28,149	69,407
Gasoline / Natural Gas (Bi-fuel)	100,412	27,720	24,159	31,724	184,015
Hybrid Electric (HEV)	295,043	413,542	588,476	780,294	2,077,355
Plug-in Hybrid (PHEV)	192,851	210,055	524,200	1,258,570	2,185,676
Battery Electric (BEV)	669,675	919,567	2,383,991	3,974,420	7,947,653
Other	14,561	5,688	855	505	21,609
Total	20,543,261	19,117,635	20,428,620	19,932,190	80,021,708

Notes: This table reports registered new vehicle sales in China between 2019 and 2022, aggregated from monthly registration records. Hybrid Electric Vehicles (HEV), Plug-in Hybrid Electric Vehicles (PHEV), and Battery Electric Vehicles (BEV) are reported as separate categories following the raw fuel-type classification in the data. Other includes Fuel Cell Vehicles (FCV) and methanol vehicles. The Total column reports the sum across years.

4.2 Power Plants in China

Data on coal-fired power plants are obtained from the *Global Energy Monitor (GEM)* database, which provides comprehensive, plant-level information on operational status, geographic coordinates, installed capacity, and primary fuel type. We restrict our analysis to utility-scale thermal power plants that were operational during the study period. These plants account for the overwhelming majority of fossil-based electricity generation in China and therefore represent the primary source of marginal emissions relevant for EV charging. We also use other types of power plants as placebo tests.

We use the precise latitude and longitude coordinates reported in GEM to construct geospatial measures of local pollution exposure. Specifically, we generate buffers with a 10-kilometer and 20-50-kilometer radius around each power plant, a distance widely used in the environmental justice and pollution epidemiology literature to capture population exposure to power plant emissions. These buffers allow us to characterize the communities that are most directly affected by pollution from coal-fired generation. We further match these geospatial buffers to gridded satellite observations of NO_2 and SO_2 to measure monthly plant-level emission intensity and downwind pollution transport.

By linking EV adoption in cities to pollution outcomes in locations near power plants, we can directly examine whether EV-induced electricity demand shifts environmental burdens from urban vehicle users to the communities surrounding coal-fired electricity generation. The spatial granularity of the GEM dataset enables us to identify which populations are affected precisely and to quantify the extent of pollution redistribution across space.

4.3 Satellite Data

Air Pollutants. Our air pollution data come from two sources. The first source is ground-level monitoring station data at the city level. We obtain hourly NO_2 concentrations from the National Urban Air Quality Real-time Publishing Platform of the China National Environmental Monitoring Center. We aggregate these station-level data to the city-month level for the period 2019-2022. The second source is satellite remote sensing data. We utilize the tropospheric vertical column density of nitrogen dioxide (NO_2) from the Sentinel-5P TROPOMI satellite. NO_2 is a short-lived pollutant highly correlated with fossil fuel combustion. TROPOMI offers a substantial improvement over previous instruments with a spatial resolution of approximately 3.5×7 km, allowing us to detect pollution plumes from individual power complexes.

To distinguish coal combustion from traffic emissions, we also extract Sulfur Dioxide (SO_2) concentrations from TROPOMI. Since gasoline vehicles emit negligible sulfur, SO_2 serves as a *"chemical fingerprint"* for coal-fired power generation. We also examine ground-level ozone (O_3), a secondary pollutant formed through photochemical reactions involving nitrogen oxides and volatile organic compounds under sunlight. O_3 is not emitted directly at the source but forms downwind and can persist over longer distances.

To capture the broader welfare and environmental justice implications, we supplement our analysis with ground-level concentrations of Fine Particulate Matter ($PM_{2.5}$). Unlike NO_2 and SO_2, which serve as direct tracers of immediate smokestack emissions, $PM_{2.5}$ is largely a secondary pollutant formed through the atmospheric oxidation of precursors (including SO_2 and NO_x). We utilize high-resolution monthly $PM_{2.5}$ grids derived from satellite Aerosol Optical Depth (AOD) retrievals fused with ground-based monitoring data via machine learning algorithms. This variable allows us to measure the aggregate health exposure facing communities downwind of the power plants, capturing both the primary soot and the secondary particles formed during plume transport.[8]

Meteorological Data and Wind Direction. To implement our wind-direction identification strategy, we integrate meteorological data from the ECMWF ERA5-Land monthly reanalysis dataset. This dataset provides hourly estimates of the direction components of wind at 10 meters above the surface, with a spatial resolution of 9 km.

For every plant-month observation, we calculate the dominant wind vector. We then

[8]AOD is a dimensionless measure of the amount of light absorbed or scattered by particles in the atmosphere. While meteorological factors (e.g., humidity, boundary layer height) affect the ratio between column AOD and ground-level $PM_{2.5}$, our inclusion of extensive fixed effects (City $\times$ Month) and meteorological controls (PBLH, precipitation) effectively absorbs these vertical profile variations, allowing AOD to serve as a valid proxy for ground-level pollution changes driven by power generation (Lyapustin et al., 2018).

dynamically partition the area surrounding each power plant into two sectors: the downwind sector and the upwind sector. This geometric construction allows us to compare pollution levels in the plume's path against the upwind *placebo* direction, differencing out direction-invariant confounders such as local traffic or economic activity.[9]

4.4 Air Pollution Monitoring Station Data

We collect ground-based air pollution data from monitoring stations for the period 2016 to 2022.[10] These data include particulate matter ($PM_{2.5}$ and PM_{10}), nitrogen dioxide (NO_2), sulfur dioxide (SO_2), carbon monoxide (CO), ozone (O_3), and the Air Quality Index (AQI), a composite measure that aggregates information across all criteria pollutants. We aggregate hourly observations to monthly averages at the station level to match the timing of EV adoption data and to reduce short-term measurement error.

4.5 Electricity Generation and Power Grid Mapping

We collect the electricity generation and infrastructure distribution from the *Compilation of Electricity Industry Statistical Data*. Electricity is transmitted across regions, so linking city-level EV adoption to plant-level emissions requires modeling the structure of China's power grid. We construct weights w_{pc} that represent the share of electricity generated by the plant p that is allocated to the city c. These weights combine engineering, geographic, and institutional information and are essential for mapping marginal electricity demand from EV charging to marginal emissions at coal-fired power plants.

The construction of w_{pc} relies on three data components. First, we incorporate detailed information on the topology of transmission lines and substations from the *State Grid Corporation*, which identifies the feasible physical paths through which electricity can flow. Second, we use provincial dispatch rules and interconnection arrangements that govern how electricity is prioritized and traded across regions. Third, we integrate technical characteristics, such as the rated capacity and directionality of cross-provincial ultra-high voltage (UHV) lines, because these corridors dominate long-distance transmission and thereby shape the marginal supply response to EV demand.

To ensure robustness, we construct several alternative weighting schemes, including

[9] We extract the Planetary Boundary Layer Height (PBLH) to control for atmospheric stability, as a lower boundary layer can trap pollutants and mechanically increase concentration readings.

[10] Because high-resolution Sentinel-5P satellite data are available only from 2019 onward, we use monitoring station data to conduct robustness checks and extend the analysis to earlier years, when EV penetration was still limited. This independent data source allows us to validate the satellite-based results and assess the relationship between EV adoption and air quality over a longer time horizon.

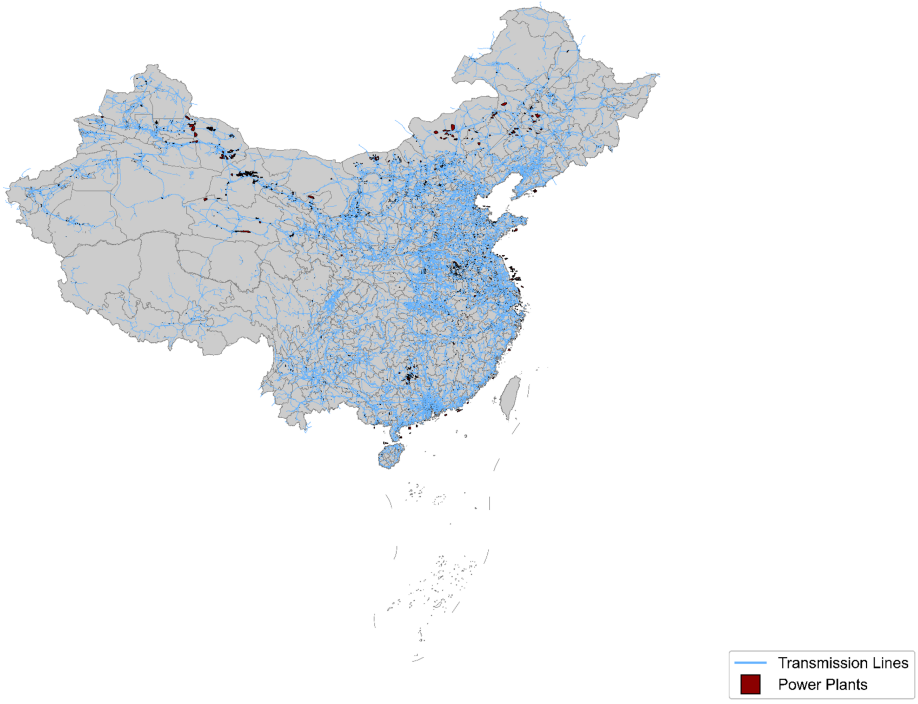


Figure 3: China Power Grid Network and Power Plants in 2022

Notes: The map illustrates the power grid network within the study area. The blue lines represent transmission lines, and the red stars indicate the locations of power plants. The map projection has been adjusted to minimize high-latitude distortion.

distance-based kernels, network-flow approximations, and allocations proportional to provincial generation shares. Our identification strategy also exploits discontinuities at dispatch and balancing boundaries, which generate sharp changes in the likelihood that a given city is served by a particular power plant, even when geographic distance varies smoothly, following the approach developed by Arkolakis and Walsh (2023). These boundaries offer a quasi-experimental source of variation in plant-city connectivity that strengthens the causal interpretation of our results.

Figure 3 visualizes the resulting grid network, showing major transmission corridors and the geographic distribution of power plants in 2022. The map shows the extensive reach of the UHV network and the importance of accounting for long-distance power flows when evaluating the environmental consequences of EV adoption.

4.6 Other Supplementary Data

Socioeconomic Characteristics. To evaluate environmental justice implications, we construct a comprehensive dataset of community attributes at the city level. We source data from the *China City Statistical Yearbook*, which serves a dual purpose: it provides a rich set of time-varying city-level control variables for our baseline specification, and supplies key economic and infrastructure metrics, such as GDP per capita, urban development, and healthcare availability, to identify vulnerable regions. We complement this with demographic characteristics, specifically educational attainment and age structures, obtained from the 2020 Population Census. We leverage these specific indicators to explicitly define *disadvantaged communities* across multiple dimensions, allowing us to test whether the pollution costs of EV adoption are regressively distributed towards populations characterized by economic fragility, resource scarcity, and demographic vulnerability.

Weather and Other Controls. We merge high-frequency weather data from the weather forecasts, including temperature, humidity, wind speed and direction, and planetary boundary layer height. These variables are critical to controlling for atmospheric dispersion. We also control for industrial output, population, and contemporaneous environmental regulations such as vehicle emission standard upgrades and coal-to-gas transitions.

4.7 Summary Statistics

Table 2 reports descriptive statistics for the key variables used in the city-level and plant-level analyses. The city-month sample has an average NO_2 concentration of 22.6 with substantial cross-city variation, while EV adoption remains limited during the sample period, with a mean EV share of 0.5 percent, reflecting the early stage of diffusion before 2022. Meteorological variables display the expected dispersion across locations and seasons, and economic controls, including GDP per capita, population, and secondary-industry share, exhibit considerable heterogeneity where available. The plant-level sample links communities surrounding power plants to satellite-based pollution measures by distance and wind direction. Average EV penetration is 0.78, mean NO_2 within 10 km of plants is 4.32 and is higher downwind, and pollution levels decline at larger downwind distances, consistent with atmospheric dispersion. SO_2 and O_3 also vary substantially, reflecting coal combustion intensity and photochemical formation processes.

Table 2: Summary Statistics of Key Variables in the Empirical Analysis

Panel A: City-level Regression						
Variable	Observations	Mean	Std. Dev.	Min	Max	Median
NO_2 mean	28,158	22.642	10.498	5.415	86.838	20.030
EV shares of sales	28,158	0.005	0.034	0	1	0
Wind speed	28,158	5.082	1.169	1.727	11.300	5.036
Pressure	28,158	933.946	97.841	542.057	1,031.469	973.278
Temperature (K)	28,158	286.710	10.695	-210.000	304.676	288.338
Humidity (%)	28,158	63.190	15.006	13.044	93.362	66.276
ln(GDP per capita)	17,604	10.952	0.513	9.367	12.460	10.910
Share of manufacturing GDP (%)	17,604	41.421	10.324	10.600	73.030	41.790
ln(Population)	17,604	5.871	0.752	3.045	8.137	5.945
Panel B: Plant-level Regression						
Variable	Observations	Mean	Std. Dev.	Min	Max	Median
EV penetration	252,840	0.008	0.040	0	0.905	0
Gasoline hybrid penetration	252,840	0.004	0.017	0	0.245	0
Fuel Vehicle (FV) penetration	252,840	0.777	0.344	0	1	0.938
NO_2 10km	252,840	4.322	3.591	0	37.944	3.136
NO_2 10km upwind	252,117	4.247	3.586	0	38.732	3.058
NO_2 10km downwind	252,260	4.398	3.652	0	39.425	3.195
NO_2 20–50km downwind	252,535	3.714	3.266	0	30.445	2.610
SO_2	216,780	19.765	24.087	0.000	732.867	19.765
O_3	253,297	0.138	0.016	0.100	0.204	0.135

Notes: This table reports summary statistics for variables used in the city-level and plant-level regressions. Observations vary across variables due to differences in data availability and sample restrictions. Pollution variables come from Sentinel-5P and related satellite products; EV penetration measures are constructed from monthly new energy vehicle registration data.

5 Empirical Strategy

This section presents the empirical strategy used to identify the causal effect of electric vehicle (EV) adoption on the spatial distribution of air pollution in China. The analysis separates reductions in on-road tailpipe emissions from increases in upstream smokestack emissions at electricity-generating facilities. We first estimate the effect of EV adoption on urban air quality in road-adjacent grids, then examine pollution responses in communities surrounding coal-fired power plants supplying electricity to high-adoption cities, and finally assess whether the resulting pollution redistribution disproportionately affects certain groups of people.

5.1 The Tailpipe Effect at the City Level

We begin by documenting the direct consumption-side benefits of electrification, what we refer to as the *tailpipe effect.* We examine whether greater local EV penetration reduces

total ambient urban air pollution. Thus, we estimate the following city-by-month panel specification:

$$P_{ct} = \alpha + \beta^{\text{local}} \times EVShare_{ct} + \mathbf{X}'_{ct}\gamma + \delta_c + \lambda_t + \epsilon_{ct}, \tag{1}$$

where P_{ct} denotes the mean concentration of various pollutants in city c during month t. The variable of interest, $EVShare_{ct}$, is defined as the ratio of new EV registrations to total vehicle registrations. The vector $\mathbf{X}_{ct}$ includes time-varying controls such as temperature, precipitation, wind speed, and local industrial activity proxies. We include city fixed effects δ_c to control for time-invariant urban characteristics and month-of-sample fixed effects λ_t to absorb national seasonality and trends.

Under this specification, the coefficient β^{local} captures the change in local air pollution associated with a greater share of EV adoption. A negative and statistically significant β^{local} indicates that EV uptake reduces urban pollution concentrations, consistent with the removal of tailpipe emissions from densely populated areas.

5.2 The Smokestack Effect at Power Plants

Identifying pollution generated by coal-fired power plants is challenging because observed emissions reflect a combination of local traffic, industrial activity, and meteorological patterns. Additionally, omitted variable bias arises when unobserved factors, such as local economic growth, simultaneously drive both higher EV adoption and increased air pollution due to higher incomes and greater environmental awareness in urban areas. To isolate the marginal pollution plume attributable to electricity generation, we implement an approach that compares local pollution across zones differentially exposed to the same plant's emissions while holding all city-level shocks constant.

For each power plant i, we classify surrounding areas into three distance bands based on the location of monitoring grids relative to the plant centroid. The *Near Zone* includes locations within 0-10 km of the plant, the area most exposed to high-stack emissions. The *Buffer Zone* includes locations 10-20 km away, capturing intermediate exposure. The *Control Zone,* defined as 20-50 km from the plant, serves as a local counterfactual that shares the same general environment but is far less directly exposed to the concentrated thermal plume. These distance bands exploit the well-documented spatial decay of power-plant emissions and enable a within-plant comparison that differentiates out broader regional confounders. We estimate the following specification at the plant–band–month level:

$$P_{idt} = \sum_{k \in \{Near, Control\}} \beta_k \left(\mathbb{1}[Bin_d = k] \times EVPen_{c(i)t} \right) + \mu_{id} + \phi_t + \nu_{idt}. \tag{2}$$

where P_{idt} measures pollution concentration in distance band d around power plant i in month t. We also report specifications using the logarithm of air pollution as an alternative outcome measure. $EVPen_{c(i)t}$ represents the EV penetration in city c that is electrically connected to power plant i. The summation $\sum_{k \in \{Near, Control\}}$ is taken over distance bins around each power plant. Since each observation belongs to a single distance bin, the summation effectively selects either the Near or the Control interaction in each observation.

Because electricity dispatch operates over large geographic areas, generation at a given power plant may respond to EV charging demand originating in distant cities. For example, a coal-fired plant located in Hebei can increase output in response to EV adoption in Beijing. To reflect this institutional feature, the EV penetration variable used in the regression, $EVPen_{ct}$, is constructed as a transmission-weighted measure of EV adoption across electricity-demand cities connected through the power grid.

$$EVPen_{ct} = \sum_j ShareOut_{c,j,\text{base}} \times VehicleShare^{EV}_{j,t}, \tag{3}$$

where $ShareOut_{c,j,\text{ base}}$ represents the baseline proportion of electricity generated in city c that is dispatched to city j. This measure ensures that our treatment captures the demand-side pull that distant EV adoption exerts on local power plant production. Using the same transmission weights, we also construct analogous measures for fuel vehicles and hybrid vehicles, which are used in supplementary analyses.

Power plant-by-distance fixed effects μ_{id} absorb time-invariant factors such as topography, baseline land use, and long-run industrial structure. The identifying variation, therefore, comes from comparing how pollution evolves near a plant relative to its local periphery as grid-wide EV demand fluctuates. Standard errors are clustered at the city level to accommodate spatial autocorrelation among nearby grids. We also control city-by-time fixed effects η_{ct} in robustness checks to absorb all shocks common to the city in which the plant is located, including weather fluctuations, regional economic cycles, and transportation activity.

The coefficient β_{Near} captures the change in pollution within 10 km of the power plant in response to an increase in EV adoption. A positive value implies that EV diffusion widens the pollution gradient around coal-fired generation, providing causal evidence of the *smokestack effect.*

A potential concern is that EV adoption may be endogenous to unobserved determinants of pollution. We address this in three ways. First, we instrument for $EVPen_{ct}$ using the

staggered introduction of local EV charging-infrastructure mandates. These policy shocks generated sharp and plausibly exogenous variation in EV adoption across cities. Second, we include controls for contemporaneous national environmental regulations, including revisions to vehicle emission standards, the COVID-19 effect, and the heating period in winter. Third, we conduct a series of placebo tests exploiting heterogeneity in plants' exposure to EV-driven electricity demand. Specifically, we compare plants with different degrees of connection to EV-intensive cities, examine heterogeneous responses across generation technologies, and leverage dispatch-boundary discontinuities that generate sharp differences in the marginal electricity mix across adjacent locations.[11]

6 Main Results

6.1 The Tailpipe Effect of Pollution Reduction

Table 3 reports city-by-month regressions of monthly average NO_2 on EV adoption using the data from 2019 to 2022. Column (1) includes only city and year-month fixed effects, so identification comes from within-city changes in EV share over time relative to the national month shocks. The estimated coefficient on $EVshare$ is negative and marginally significant, consistent with the view that electrification of the vehicle fleet reduces traffic-related NO_2. Column (2) adds a rich set of meteorological controls (wind speed, pressure, temperature, and humidity), which absorb a major source of high-frequency variation in ambient NO_2. The magnitude becomes larger in absolute value.

Column (3) further introduces time-varying economic controls, including log GDP per capita, the industrial GDP share, and log population, to proxy for shifts in local activity and structural change that may co-move with EV adoption. The coefficient on $EVshare$ remains negative and statistically significant, with a magnitude close to Column (1). The stability of the estimate across Columns (1)-(3) suggests that the negative association is not mechanically driven by observable changes in the local economic environment.

Column (4) allows the effect of EV adoption to vary with road density, which proxies for traffic intensity and baseline exposure to tailpipe emissions. The coefficient on $EVshare$ captures the effect of EV adoption in cities with below-median road density, where traffic-related emissions are relatively less important, and is statistically insignificant. In contrast, the interaction between $EVshare$ and $Road$ is negative and statistically significant, indicat-

[11] Figure A.2 illustrates the identification strategy. Panel 1 shows the empirical design, comparing locations near coal-fired power plants to farther locations that serve as a local counterfactual. Panel 2 summarizes the regression implications: increased EV adoption raises grid load and induces a larger pollution response in the near zone as captured by Equation (2). Panel 3 presents a wind-direction falsification test.

Table 3: Effect of EV Adoption on City-level NO_2

	NO_2 mean (monthly average)			
	(1)	(2)	(3)	(4)
EV share	-1.5118*	-2.0311**	-1.4321*	2.6693
	(0.8741)	(0.8357)	(0.8259)	(1.8362)
EV share×Road				-4.7787**
				(1.8444)
Road				-0.5935**
				(0.2983)
Wind speed		-1.1849***	-1.1010***	-1.1011***
		(0.0856)	(0.0893)	(0.0894)
Pressure		0.5660***	0.6029***	0.6024***
		(0.0286)	(0.0334)	(0.0336)
Temperature		-0.1877***	-0.2014***	-0.2022***
		(0.0378)	(0.0396)	(0.0397)
Humidity		-0.1617***	-0.1586***	-0.1585***
		(0.0091)	(0.0090)	(0.0090)
ln(GDP per capita)			0.9016	0.8366
			(0.8025)	(0.8051)
Industrial GDP share			0.0235	0.0246
			(0.0252)	(0.0253)
ln(Population)			-4.2509	-4.3398
			(2.7822)	(2.7255)
Constant	22.6504***	-435.8653***	-463.7954***	-461.6801***
	(0.0046)	(30.6897)	(36.1710)	(36.3040)
City FE	Yes	Yes	Yes	Yes
Year-month FE	Yes	Yes	Yes	Yes
Observations	28,158	28,158	17,604	17,580
R^2	0.8519	0.8919	0.8915	0.8917

Notes: The dependent variable is the monthly NO_2 concentration at the city level. All specifications include city and year-month fixed effects. Standard errors are reported in parentheses and are clustered at the city level. *, **, and *** indicate significance at the 10%, 5%, and 1% levels, respectively. *Road* is a dummy variable, which equals 1 if a city's highway mileage exceeds the sample median and 0 otherwise. Highway mileage data is from the China City Statistical Yearbook.

ing that the pollution-reducing effect of EV adoption is concentrated in cities with denser road networks. Quantitatively, EV adoption leads to a significantly lower by around 4.78% in NO_2 in high-road-density cities compare to its counterparts, consistent with EVs displacing combustion vehicles precisely where traffic emissions are most intensive. This pattern supports the interpretation that EV adoption operates as an effective abatement margin in urban environments, rather than merely proxying for broader economic or infrastructural changes.

6.2 The Smokestack Effect of Pollution Reallocation

Then we shift the focus from urban centers to the areas surrounding coal-fired power plants, revealing a critical and underexplored dimension of the EV transition. Table 4 reports baseline estimates of the relationship between EV adoption and NO_2 concentrations measured within a 10 km radius of power plants. Across all specifications, higher EV penetration is associated with statistically significant increases in local NO_2 exposure. In Columns (1) and (2), a one-unit increase in EV penetration raises NO_2 levels by about 0.42-0.43 units, with estimates stable after conditioning on a full set of meteorological controls. Columns (3) and (4) yield consistent results in logarithmic terms: EV penetration increases log NO_2 by roughly 2.0-2.2%, again robust to weather controls. The precision of the estimates and their insensitivity to additional covariates suggest that the results are not driven by confounding short-run meteorological variation.[12]

These findings provide clear evidence of a spatial reallocation of pollution rather than an unambiguous reduction. While EV adoption is often justified by reductions in tailpipe emissions, the plant-level results indicate a corresponding increase in emissions exposure near electricity generation sites. Because all specifications include plant fixed effects and year-month fixed effects, identification comes from within-plant changes over time, net of common shocks and persistent plant characteristics. The magnitudes are economically meaningful given the scale of EV adoption in China and the large populations residing near thermal power plants.

The results have several policy implications for environmental justice and policy design. Without parallel investments in grid decarbonization, the rapid deployment of EVs risks exacerbating local pollution burdens in already vulnerable areas, even as it delivers aggregate environmental benefits. The estimates provide direct empirical evidence of this spatial redistribution mechanism. A natural next question is whether this reallocation depends on the structure of the electricity network itself. In particular, to what extent do transmission constraints and inter-regional power flows mediate the link between EV demand and plant-level emissions, and how much of the observed effect is driven by EV adoption in other cities versus demand originating in distant urban centers but within city? Addressing these questions is essential for understanding how infrastructure and market integration shape the distributional consequences of green transportation policies.

[12]Our estimates do not explicitly account for green electricity or renewable charging requirements associated with EV adoption. To the extent that a portion of EV-induced electricity demand is met by cleaner generation sources, the estimated pollution displacement effects should be interpreted as conservative, lower-bound measures of the pollution that would arise under a fully coal-based marginal electricity supply (Xinhua News Agency, 2025).

Table 4: Baseline Results for EV Adoption on Plant-Level NO_2 (10 km Radius)

	NO_2 (10 km)		$\ln(NO_2)$ (10 km)	
	(1)	(2)	(3)	(4)
EV penetration	0.4209***	0.4325***	0.0204*	0.0221**
	(0.1126)	(0.1130)	(0.0109)	(0.0109)
Wind speed		-0.2260		-0.0043
		(4.4085)		(0.4813)
Pressure		0.2320		0.0276
		(0.6730)		(0.0783)
Temperature		-0.0005		-0.0001
		(0.0009)		(0.0001)
Humidity		-0.0290		-0.0056
		(0.0307)		(0.0036)
Constant	4.3187***	4.2322***	1.4926***	1.4740***
	(0.0039)	(0.1816)	(0.0004)	(0.0177)
Plant FE	Yes	Yes	Yes	Yes
Year-month FE	Yes	Yes	Yes	Yes
Observations	252,840	250,838	252,840	250,838
R^2	0.7600	0.7600	0.8805	0.8805

Notes: The dependent variable is the monthly NO_2 concentration measured within a 10 km radius of each plant. Columns (2) and (4) additionally include weather controls (wind speed, pressure, temperature, humidity). All specifications include plant and year-month fixed effects. Standard errors are in parentheses and clustered at the city level. *, **, and *** denote significance at the 10%, 5%, and 1% levels.

7 Robustness Checks

7.1 Wind-Adjusted Pollution Exposure

To disentangle the pollution plume generated by power plants from ambient urban background pollution, we leverage high-resolution meteorological data from the ERA5 monthly reanalysis dataset produced by the ECMWF.[13] For each power plant i in month t, we extract the 10-meter zonal (u) and meridional (v) wind components to calculate the dominant monthly wind vector. This allows us to identify the spatial direction of pollutant dispersion.[14]

We define the *downwind zone* as the spatial wedge extending from the power plant aligned with the wind vector. Specifically, we calculate the bearing angle from the plant's centroid to each grid cell within a 50 km radius. A grid cell is classified as *downwind* if its bearing

[13]ERA5 is the fifth generation of atmospheric reanalysis data produced by the European Centre for Medium-Range Weather Forecasts (ECMWF), providing comprehensive global weather data. Reanalysis combines historical observations with modern weather models to produce consistent and high-resolution datasets, widely used in environmental and economic research.

[14]The zonal wind component (u) represents the east-west direction, with positive values indicating wind blowing from west to east. The meridional wind component (v) represents the north-south direction, with positive values indicating wind blowing from south to north. Together, these components define the wind vector and its direction.

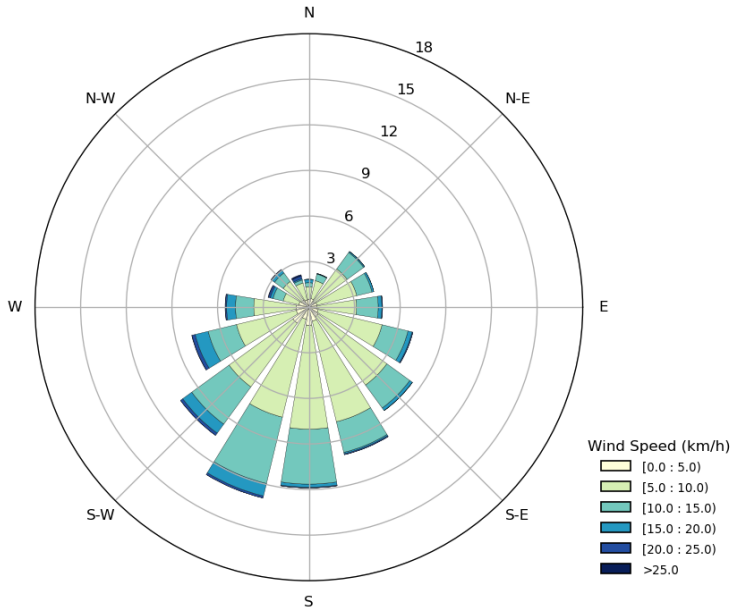


Figure 4: Wind speed and direction distribution for Anhui Bengbu Power Station (2019)

Notes: This figure illustrates the wind rose for the Anhui Bengbu Power Station (Phase II, Unit 3), located in Huaiyuan County, Bengbu City, Anhui Province (32.78°N, 117.11°E). The plant is a 660 MW ultra-supercritical coal-fired unit fueled by bituminous coal, which commenced operations in 2018. The map is based on hourly wind vector data (10 m above ground level) retrieved from the ERA5-Land reanalysis dataset for the year 2019. Wedges indicate the frequency of wind direction, while colors represent wind speed intervals (km/h).

angle lies within $\pm 45°$ of the wind vector, creating a 90° cone. This zone captures the area most affected by emissions transported by prevailing winds.

Conversely, the *upwind zone* is defined as the opposing 90° cone ($180° \pm 45°$ relative to the wind vector). This zone serves as a counterfactual, as it shares the same local economic geography and land-use characteristics as the downwind zone but is shielded from the plant's emissions due to meteorological transport. By comparing pollution levels between these zones, we can isolate the causal impact of power plant emissions. Appendix B shows more details on the wind adjustment pollution construction.

Table 5 investigates the robustness of the observed plant-level NO_2 effects by incorporating wind-direction adjustments to distinguish between upwind and downwind exposure. If the baseline estimates in Table 4 were driven by spurious spatial correlations or measurement artifacts, we would expect the relationship between EV penetration and NO_2 to attenuate or vanish once wind direction is accounted for. Instead, the results demonstrate that EV penetration remains positively and significantly associated with NO_2 concentrations in downwind areas, reinforcing the evidence for the pollution displacement mechanism. Conversely, the significant negative difference observed in the upwind direction serves as a critical falsifica-

tion test; it indicates that pollution levels are lower in the immediate vicinity of the plant compared to distant upwind areas, effectively ruling out omnidirectional confounders that would generate uniform effects regardless of wind direction.

Panel A documents the effects in downwind areas, where prevailing winds carry power plant emissions toward nearby communities. The results reveal a clear distance-decay pattern consistent with the atmospheric dispersion of point-source emissions. EV adoption increases NO_2 by 0.34 $\mu g/m^3$ within the 0–10 km zone, declining monotonically to 0.19 $\mu g/m^3$ in the 20–50 km band. Column (5) quantifies this gradient by differencing NO_2 exposure between the near-plant (0–10 km) and outer (20–50 km) zones. The positive coefficient confirms that pollution concentrations are highest near the source and dissipate with distance, validating the pollution displacement mechanism.

Panel B presents upwind results, in which prevailing winds carry emissions away from the measured locations. Strikingly, the spatial gradient operates in the opposite direction. Columns (1)-(4) show that EV adoption increases NO_2 concentrations by 0.48 $\mu g/m^3$ in the 0-10 km upwind zone, with the effect rising to 0.76 $\mu g/m^3$ in the 20-50 km band, indicating an inverted spatial pattern in which pollution effects are larger at greater distances. Column (5) formalizes this reversal: the upwind spatial gradient is negative and significant, indicating that areas farther upwind experience substantially greater pollution increases than those in the plant's immediate vicinity.

This opposing spatial structure, with distance decay in downwind areas versus distance accretion in upwind areas, provides critical evidence for our identification strategy. The inverted upwind gradient reflects the strategic rural-urban siting of power plants, as discussed in Morehouse and Rubin (2021). In China, power plants are typically situated in suburban or rural areas, positioned downwind of the population centers they serve to mitigate urban exposure. Consequently, the immediate upwind zone (0-10 km) often comprises a *rural or semi-urban buffer* with lower baseline activity. In contrast, the distant *upwind 20-50 km* zone likely captures the *urban core* that generates electricity demand from EV adoption. The large coefficient in this distant upwind zone thus aggregates the effects of concentrated urban electricity demand, whereas the immediate upwind zone reflects the quieter rural surroundings.

These findings provide a powerful falsification test. Under spurious spatial correlations, such as regional economic booms, pollution coefficients would rise uniformly around the plant. The observed asymmetry between the downwind area within 10 kilometers of the plant and the upwind demand center located 20 to 50 kilometers away instead rules out omnidirectional confounders.

The key policy implication is that *downwind communities bear concentrated, localized*

Table 5: Effect of EV Adoption on NO_2 by Wind Direction and Distance

	(1) 0–10 km	(2) 0–20 km	(3) 0–50 km	(4) 20–50 km	(5) diff. (0–10 km - 20–50 km)
Panel A: Downwind					
EV penetration	0.3386***	0.2909**	0.2133**	0.1867*	0.1595***
	(0.1158)	(0.1122)	(0.1068)	(0.1059)	(0.0591)
Constant	4.2253***	3.9968***	3.6593***	3.2613***	0.6408***
	(0.1874)	(0.1757)	(0.1723)	(0.6629)	(0.1038)
Observations	250,269	251,066	252,163	251,066	250,269
R^2	0.7615	0.7579	0.7478	0.7457	0.4712
Panel B: Upwind					
EV penetration	0.4763***	0.5606***	0.7218***	0.7592***	-0.2890***
	(0.1144)	(0.1150)	(0.1127)	(0.1127)	(0.0500)
Constant	4.2544***	4.0277***	3.4527***	3.3827***	0.9087***
	(0.1854)	(0.1685)	(0.1538)	(0.1520)	(0.0994)
Observations	250,118	250,847	252,155	250,847	250,118
R^2	0.7435	0.7303	0.7061	0.7015	0.5281
Weather controls	Yes	Yes	Yes	Yes	Yes
Plant FE	Yes	Yes	Yes	Yes	Yes
Year-month FE	Yes	Yes	Yes	Yes	Yes

Notes: This table presents the effect of EV adoption on NO_2 concentrations at varying distances from power plants, separately for downwind and upwind directions. Columns (1)–(4) report results for 0–10 km, 0–20 km, 0–50 km, and 20–50 km zones. Column (5) reports the difference between the 0–10 km and 20–50 km zones. All specifications include weather controls, plant fixed effects, and year-month fixed effects. Standard errors in parentheses are clustered at the city level. *, **, and *** indicate significance at the 10%, 5%, and 1% levels.

pollution burdens. The significant downwind gradient demonstrates that EV adoption creates a sharp pollution spike within 10 km of power plants. This asymmetry underscores a critical environmental justice dimension: the costs of vehicle electrification are physically displaced from the urban centers (located upwind) to the rural or suburban communities immediately downwind of coal-fired infrastructure.

7.2 Shift-Share Instrumental Variables Design

A key concern in identifying the causal effect of EV adoption on pollution is the potential endogeneity of EV sales. Regional EV demand may be correlated with unobserved regional economic conditions in the error term (ϵ_{idt}), such as income growth or industrial activity, which could independently influence electricity consumption and pollution. As a result, OLS estimation may be biased upward, conflating the effect of EV adoption with broader economic trends.

To address this challenge, we construct a Shift-Share Instrumental Variable that leverages

exogenous variation in EV adoption driven by the interaction of local supply-side factors and national demand shocks. Specifically, we predict regional EV demand using the following shift-share formula:

$$Z_{ct} = \sum_{c \in r} \left(Chargers_{c,base} \times \ln(NationalEVSales_{-c,t}) \right), \tag{4}$$

where $Chargers_{c,base}$ represents the density of public charging stations in city c in the 2019 base year. This variable captures the pre-existing local capacity to support EV adoption, which was largely determined by administrative mandates and infrastructure planning rather than contemporaneous economic activity. $NationalEVSales_{-c,t}$ denotes the aggregate national EV sales in month t, excluding city c. This term captures exogenous temporal variation in EV adoption driven by national policy changes and technological advancements.

The validity of this instrument relies on the exclusion restriction, which requires that the interaction of baseline charging infrastructure and national EV sales trends affects local pollution only through its impact on local EV adoption and the resulting electricity demand. This assumption is plausible because the baseline distribution of charging stations was determined by long-term infrastructure planning rather than short-term industrial activity or pollution levels. Moreover, national EV sales trends are driven by factors such as subsidy phase-outs and technology diffusion, which are orthogonal to local economic shocks. By isolating variation in EV adoption that is plausibly exogenous to local economic conditions, the shift-share IV provides a robust strategy to address endogeneity concerns.

Table 6 shows the estimation results of both the OLS and IV estimators. Columns (1) and (2) report OLS benchmarks. In Column (1), which includes power plant fixed effects, province-by-year fixed effects, and weather controls, a 1 unit increase in EV penetration is associated with a 0.44 increase in NO_2 concentrations near power plants. Column (2) controls for year-month fixed effects and adds local economic controls. The coefficient declines modestly to 0.37 but remains highly significant.

Columns (3) and (4) present the two-stage least squares results. The first stage in Column (3) shows that the log number of public charging stations is a strong predictor of EV penetration, with a coefficient of 0.0003. The corresponding Cragg-Donald Wald F-statistic of 53.68 comfortably exceeds conventional weak-instrument thresholds, confirming the relevance of the instrument. Importantly, charging infrastructure expansion has no statistically meaningful association with local GDP, income, or industrial structure once fixed effects are included, supporting the plausibility of the exclusion restriction.

The second-stage estimates in Column (4) indicate that instrumented EV penetration increases NO_2 concentrations near power plants by 0.47. This IV estimate is slightly larger

Table 6: IV Estimates for the Effect of EV Adoption on NO_2 within 10 km of Plants

	(1)	(2)	(3)	(4)
	OLS		2SLS	
Dependent variable	NO_2	NO_2	First stage: EV penetration	Second stage: NO_2
EV penetration	0.4430***	0.3726***		0.4722***
	(0.1138)	(0.1134)		(0.1166)
ln(Charging station)			0.0003***	
			(0.0000)	
ln(GDP)		0.1952**	-0.0001	-0.0082
		(0.0987)	(0.0002)	(0.0093)
ln(GDP per capita)		0.1710**	0.0003	0.0183
		(0.0821)	(0.0003)	(0.0210)
ln(Industrial share of GDP)		-0.7034***	-0.0001	-0.0099
		(0.1134)	(0.0000)	(0.0263)
Weather controls	Yes	Yes	Yes	Yes
Plant FE	Yes	Yes	Yes	Yes
Province-by-Year FE	Yes			
Year-month FE	Yes	Yes	Yes	Yes
Observations	250,452	224,688	132,602	131,212
R^2	0.7601	0.7668		
F-stat (Cragg–Donald Wald)				53.676

Notes: The dependent variable is the monthly NO_2 concentration measured within a 10 km radius of each plant in columns (1), (2), and (4). Column (3) reports the first-stage regression of EV penetration on the log number of public charging stations, ln(Charging station). All specifications include plant and year-month fixed effects and weather controls. Column (1) further includes province-by-year fixed effects. Columns (2)–(4) additionally include local economic controls: log GDP, log GDP per capita, and log secondary sector share. Column (4) reports the second-stage IV estimates. Standard errors are reported in parentheses and are clustered at the city level. *, **, and *** indicate significance at the 10%, 5%, and 1% levels, respectively.

than the OLS coefficients, suggesting that the OLS results may be biased downward, potentially due to measurement error in EV penetration or policy targeting that favors cleaner regions for early EV deployment.

The IV results could be interpreted as a causal effect of the baseline findings. By isolating variation in EV adoption driven by charging infrastructure rollout, the estimates provide strong evidence that transportation electrification increases upstream pollution exposure at electricity generation sites. This pattern is consistent with a smokestack mechanism rather than bias because of potential endogenous concerns and shows the central message of the paper: absent simultaneous decarbonization of the power sector, EV adoption reshapes the spatial distribution of air pollution, with important implications for environmental justice and the design of complementary infrastructure and energy policies.

7.3 Other Air Pollutants

Table A.1 extends the analysis to examine whether the pollution displacement associated with EV adoption is also evident in other pollutants, such as SO_2 and O_3, which are critical markers of fossil-fuel combustion and secondary pollution formation. Columns (1) and (2) report the estimated effects of EV penetration on SO_2 concentrations within 10 km of power plants and O_3 concentrations within 5 km, respectively.

In Column (1), the coefficient on EV penetration is positive and marginally significant, indicating that a 1 percentage point increase in EV penetration raises SO_2 concentrations near power plants by 2.11 units. Column (2) shows a small but statistically significant increase in ozone concentrations. A 1 percentage point increase in EV penetration raises local O_3 by 0.0065 units, consistent with enhanced ozone formation driven by higher NO_2 emissions from power plants. While the effect size is modest, the positive sign is consistent with the chemistry of ozone formation, which is influenced by the availability of NO_2 and volatile organic compounds.

Therefore, EV adoption induces a broader redistribution of pollution, not limited to NO_2. While the NO_2 results remain the most salient due to their strong spatial gradient and well-documented health impacts, the SO_2 and O_3 estimates provide additional evidence that the environmental costs of EV-induced electricity demand are multifaceted.

7.4 Other Robustness Checks

Alternative Specifications. Table A.2 shows that the estimated increase in NO_2 concentrations near power plants associated with EV adoption is robust across alternative specifications and inference procedures. We replace EV penetration with its logarithmic form in Column (1), which presents a positive and precisely estimated coefficient, indicating that the results are not sensitive to functional form. Column (2) adopts a long-difference specification linking year-over-year changes in EV penetration to changes in plant-level pollution; the estimated effect remains positive and statistically significant, suggesting that the pollution displacement persists beyond short-run fluctuations. Columns (3) and (4) address inference concerns by clustering standard errors at the plant level and the province level, respectively. Across all specifications, coefficient magnitudes and statistical significance remain stable, indicating that specific assumptions about the error structure do not significantly influence the main results.

Contemporaneous Policy. Satellite-based measures of NO_2 around power plants may respond not only to plant-level generation but also to contemporaneous policy changes and

macroeconomic shocks that affect transportation activity more broadly. A key concern is the nationwide phase-down of central NEV purchase subsidies between 2020 and 2022, with scheduled year-on-year reductions before their expiration at the end of 2022. Because this policy directly influences EV adoption and substitution away from internal-combustion vehicles, it could mechanically affect local pollution levels near plants through changes in traffic-related emissions. To address this concern, the baseline specification includes year-month fixed effects, which absorb the subsidy phase-down and other common time-varying shocks, ensuring that identification relies on cross-sectional differences in EV adoption rather than aggregate policy trends.

A second concern is the tightening of tailpipe emission standards through the staged implementation of the National VI (China 6) regime during our sample period. Recent evidence suggests these standards have measurably improved urban air quality in China (Shu et al., 2025).[15] If this regulatory tightening is not accounted for, it could bias our estimates because it may be correlated with local EV adoption, as tighter conventional standards can accelerate EV adoption while simultaneously reducing traffic-related pollutants through cleaner internal combustion engine fleets. In settings where our pollution outcome may partly capture non-power-plant sources, failing to absorb such tailpipe-standard tightening would most likely bias the EV coefficient downward, since EV growth would coincide with policy-driven reductions in local vehicle emissions. Our year-month fixed effects can also absorb the nationwide component of this regulatory tightening and related macro trends.

Beyond national policies, we explicitly address the COVID-19 pandemic as a major time-varying confounder. Pandemic-related restrictions altered travel behavior and vehicle usage, directly affecting EV adoption and charging demand, while simultaneously reshaping electricity consumption, industrial activity, and power generation. At the same time, satellite-based NO_2 measured near plants reflects not only stack emissions but also non-power-sector sources and secondary atmospheric processes, which may respond differently during localized lockdowns and abnormal meteorological conditions. If unaccounted for, city-specific pandemic shocks could induce spurious correlation between EV adoption and measured pollution. To mitigate this concern, in addition to year-month fixed effects, we include city-by-month COVID-19 controls capturing confirmed cases, deaths, recoveries, and net recoveries, which absorb heterogeneous local pandemic severity and policy stringency. The corresponding estimates are reported in Column (1) of Table 7.

Thirdly, while national EV subsidies were gradually scaled back after 2019, many cities implemented local EV incentives, such as purchase rebates, trade-in programs, and subsidies for charging infrastructure, that may be bundled with other contemporaneous city-level

[15] China 6a effective July 1, 2020, with progressively stricter requirements thereafter.

Table 7: Controlling for Contemporaneous Policies

	(1) Covid-19 Controls	(2) EV Subsidy Controls	(3) Winter Heating Period
EV penetration	0.6864***	0.3389***	0.4323***
	(0.1154)	(0.1237)	(0.1130)
ln(Case)	-0.0275		
	(0.0171)		
ln(Death)	-0.0728***		
	(0.0269)		
ln(Cure)	0.0073		
	(0.0173)		
ln(Cure new)	-0.3098***		
	(0.0154)		
Heating Dummy			0.0107
			(0.0151)
Constant	4.5540***	4.2328***	4.3103***
	(0.2415)	(0.1824)	(0.2065)
Weather controls	Yes	Yes	Yes
Plant FE	Yes	Yes	Yes
City FE	Yes	No	Yes
Year-month FE	Yes	Yes	Yes
City×Year FE	No	Yes	No
Observations	162,820	250,838	250,838
R^2	0.7570	0.7692	0.7600

Notes: The table reports fixed-effects regression estimates controlling for contemporaneous policies. Column (1) adds Covid-19 controls (log cases, deaths, cures, and new cures) to the baseline specification. Column (2) controls for EV adoption subsidies via a city-by-year fixed effects specification. Column (3) controls for winter heating policy using a heating dummy. All regressions include weather controls and the fixed effects indicated. Standard errors are reported in parentheses and are clustered at the city level. *, **, and *** denote significance at the 10%, 5%, and 1% levels, respectively.

policies affecting air quality. To remove these time-varying local confoundings, we further include city-by-year fixed effects, which absorb city-specific policy shifts and macro shocks within each year. As shown in Column (2) of Table 7, the estimates remain consistent with our main findings.

Finally, winter heating policies in northern China could confound our estimates because the statutory district-heating season sharply increases fuel combustion for space heating and heat-and-power generation, mechanically raising emissions and potentially affecting electricity demand. If EV adoption is correlated with the timing or intensity of heating, the baseline estimates may partly capture heating-driven pollution rather than EV-related charging demand.

To address this concern, we control for winter heating using a city-by-month indicator constructed from publicly available statutory heating schedules. Column (3) of Table 7 shows that the results are robust to this control, suggesting that the estimated EV-pollution

relationship is not driven by winter heating. The city-specific heating calendar used to build a dummy is reported in Table A.3.

Using Air Monitoring Station Data. Using city-level air quality monitoring data, Table A.4 provides a stringent robustness check for the main findings. Across specifications, we show that higher EV adoption is consistently associated with lower ambient pollution, as reflected in statistically significant reductions in AQI and major criteria pollutants. The effects are particularly robust for the main air pollutants, and remain significant even after controlling for province by year by month shocks, indicating that the estimates are unlikely to be driven by coincident regional trends or unobserved policy changes. Although the estimated magnitudes are smaller in the most saturated specifications, the stability of the sign and significance supports a conservative interpretation in which EV adoption leads to meaningful improvements in urban air quality.

We also analyze monitoring-station data from the early phase of EV adoption. Table A.5 reports results for stations located near power plants, distinguishing those within 10 km in Columns (1)-(3) and within 5 km in Columns (4)-(6) of at least one coal-fired facility. EV penetration is associated with statistically significant increases in NO_2, SO_2, and $PM_{2.5}$ concentrations, with estimated effects generally larger and more precisely measured at stations closer to generation sources. The consistent positive coefficients across multiple pollutants align with upstream emission responses linked to EV-related electricity demand.

To further explore spatial heterogeneity, Table A.6 examines how pollution responses vary with power plant density within 5 km. The results display a clear dose-response pattern: monitoring stations surrounded by three or more nearby plants experience the largest pollution increases in Column (1), with effect magnitudes declining as plant density falls in Columns (2) and (3). Columns (4) and (5) report placebo tests that provide additional identification evidence. For stations with no nearby plants, the baseline specification yields an insignificant coefficient in Column (4). Once province-by-year-month fixed effects are added to absorb finer spatial and temporal variation, the estimate turns negative and statistically significant in Column (5). This pattern mirrors the city-level results and supports the interpretation that the positive pollution effects observed near power plants reflect generation responses to EV-related electricity demand rather than confounding trends. Taken together with the satellite-based evidence, these findings indicate that EV adoption reallocates emissions from urban transportation toward electricity generation sites.

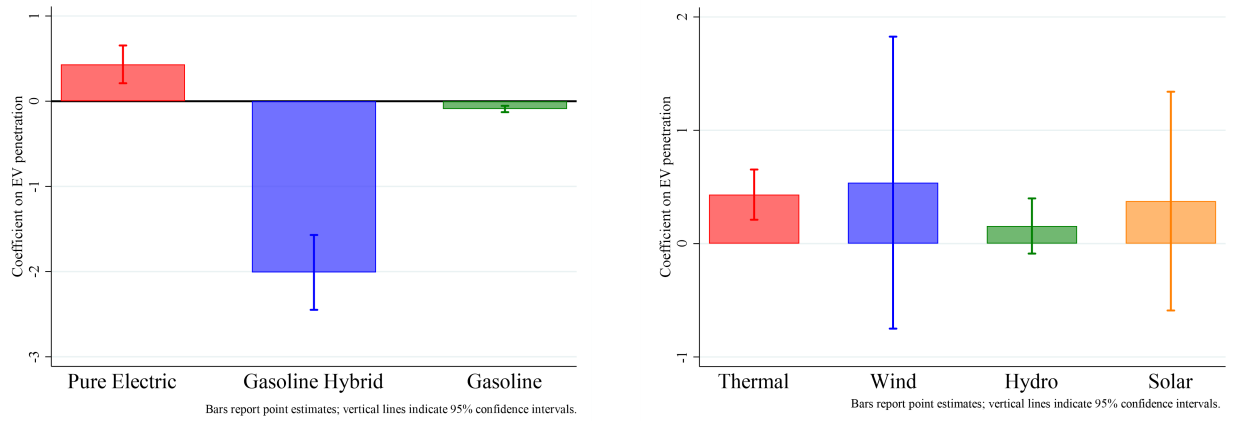
7.5 Placebo Test

Alternative Vehicle Types. Figure 5 strengthens the causal interpretation of the main findings by demonstrating that the observed increase in NO_2 concentrations near power plants is specific to EV adoption and not attributable to unrelated vehicle categories or power-plant types. Panel (a) shows the results where we replace EV penetration with two placebo measures: hybrid-vehicle penetration and fuel-vehicle penetration.[16] Neither of which should meaningfully affect electricity demand at coal-fired plants. Consistent with this expectation, both coefficients are statistically significant but negative, indicating that these vehicle types reduce tailpipe emissions without imposing additional load on the electricity grid. The contrast between these negative placebo effects and the positive EV coefficients underscores that the baseline results are not driven by mechanical correlations between vehicle adoption and local pollution.

Alternative Power Plants. Panel (b) conducts a complementary placebo test across power-plant types. As expected, EV adoption shows no significant association with NO_2 emissions in these placebo plant categories. The results indicate that pollution response is specific to electricity-generating units that plausibly supply EV charging demand. This pattern rules out explanations based on regional pollution trends or contemporaneous policies affecting all plants uniformly. Table A.8 reports placebo tests for hydropower, wind power, and solar power plants (Panels A, B, and C, respectively). We find no significant pollution displacement effects around these renewable energy facilities. Crucially, unlike the coal-fired plants where pollution effects are concentrated in downwind areas, we observe no significant effects in downwind areas at these renewable facilities, further confirming that the documented displacement effects are driven by emissions from dispatchable fossil-fuel generation rather than spurious spatial correlations.

Retired Power Plant. Figure 6 presents a final placebo test based on power plants that retired during the sample period from 2019 to 2022. Since these plants ceased operations before or during our analysis period, they no longer respond to electricity demand from EV charging. Thus, EV penetration should not affect pollution levels in their vicinity. The results confirm this expectation: the coefficients for NO_2, SO_2, and $PM_{2.5}$ are all statistically insignificant and close to zero. This finding addresses potential concerns that the baseline results might be driven by spurious correlations, such as regional pollution trends or policy changes affecting all areas with high EV adoption. If our main findings simply

[16] We show the estimation results of other types of vehicles in Table A.7.



(a) Estimation of Effects by Vehicle Type (b) Estimation of Effects by Power Plant Type

Figure 5: Placebo Tests: Alternative Vehicle Types and Power Plants

Notes: This figure reports placebo tests examining the relationship between EV penetration and outcomes that should not be directly affected by EV adoption. Panel (a) shows estimates for alternative vehicle categories, and Panel (b) shows estimates by electricity generation source. Bars report point estimates, and vertical lines indicate 95% confidence intervals. The absence of systematic effects in these placebo outcomes supports the validity of the empirical design.

reflected coincidental patterns rather than a causal supply-side response, we would still observe pollution changes near retired plants in high-EV-penetration areas. The absence of any systematic effects at these non-operational facilities strengthens the interpretation that the baseline estimates capture a genuine causal relationship between EV-induced electricity demand and emissions from active coal-fired power plants. Table A.9 shows the detailed regression results, confirming no significant pollution effects at retired power plants.

These placebo tests provide strong evidence that the observed NO_2 increases are causally linked to EV-induced electricity demand at coal-fired power plants. By isolating the effect to relevant vehicle types and generation units, the analysis highlights the interpretation of a targeted smokestack mechanism and also the importance of complementary energy-sector policies in mitigating the localized environmental costs of transportation electrification.

8 Mechanisms and Discussion

This section explores the mechanisms underlying the observed pollution redistribution effects and discusses their broader implications. We begin by examining the role of grid transmission in linking urban EV demand to peripheral power plants, highlighting how interregional electricity flows mediate the spatial distribution of environmental burdens. Next, we analyze the environmental justice implications, focusing on whether disadvantaged communities disproportionately bear the costs of increased power-plant emissions. Finally, we discuss policy

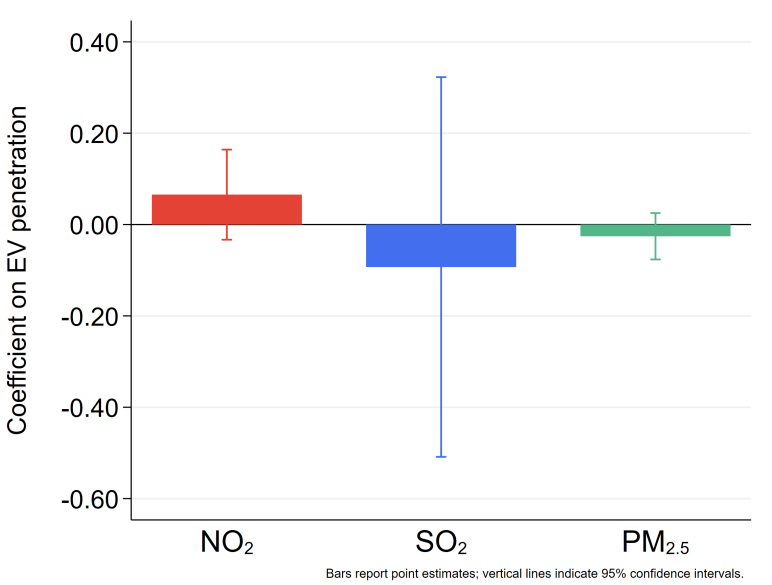


Figure 6: Placebo Test: Retired Power Plants

Notes: This figure reports a placebo test of EV penetration's effect on pollution at retired coal power plants, including all plants retired by the end of our sample period (pre-2019 and 2019–2022). For plants retiring in 2019–2022, we include only post-retirement observations. Retired plants should show no EV-related emissions response. Bars show point estimates for NO_2, SO_2, and $PM_{2.5}$, and vertical lines indicate 95% confidence intervals.

recommendations to mitigate these unintended consequences and ensure a more equitable green transition.

8.1 Grid Transmission: Decomposing EV Effects

Table 8 presents a mechanism analysis using an alternative measure of EV penetration constructed at the province level. This measure excludes the plant's own city and captures only external EV demand within the province. Following the exposure share approach in Arkolakis and Walsh (2023), this specification isolates the effect of EV adoption on power plant emissions by separating local demand from indirect exposure to EV demand elsewhere in the electricity network. This design allows us to test whether broader provincial EV adoption, driven by province level policies, infrastructure deployment, and market penetration, predicts higher NO_2 concentrations near power plants independent of a city's own EV uptake.

Columns (1) and (2) use a province-level EV penetration measure that explicitly excludes the plant's own city, capturing EV demand elsewhere in the province that may be served through grid transmission. Specifically, a 1 percentage point increase in province-level EV penetration raises NO_2 concentrations within 10 km of power plants by 0.32 units and within

20 km by 0.33 units. The stability of these results when excluding own-city EV adoption is particularly noteworthy. It partially alleviates concerns that local political campaigns or environmental initiatives targeted at cities experiencing rapid EV growth might simultaneously influence plant emissions through unrelated channels, such as enforcement intensity or technology upgrades. Instead, the findings strongly support the hypothesis that the mechanism operates through regional electricity demand rather than local confounders tied to municipal market conditions.

Column (3) isolates EV penetration within the plant's own city. The estimated coefficient is positive but substantially smaller, at 0.16 units, roughly half the magnitude of the external-demand estimates. Comparing magnitudes, roughly one-third of the total pollution response can be attributed to intra-city EV demand, while approximately two-thirds reflects inter-city electricity demand generated by EV adoption in other cities supplied by the same plants. This comparison suggests that the pollution response near power plants is driven primarily by electricity demand transmitted through the grid rather than by local EV adoption alone.

This decomposition highlights an important and often overlooked dimension of environmental justice. The pollution burden associated with EV adoption is not confined to within-city redistribution from roads to power plants. Instead, it also happens across cities through the electricity transmission network, exposing communities near power plants to emissions generated by EV demand elsewhere. As a result, the environmental costs of transportation electrification extend beyond intra-city distributional concerns to encompass inter-city inequities, showing the need for coordinated policies that jointly address vehicle electrification, grid transmission, and power sector decarbonization.

8.2 Environmental Justice

Table 9 examines whether the pollution displacement induced by EV adoption disproportionately burdens disadvantaged communities. Recent evidence suggests that differential vulnerability across socioeconomic groups can amplify well-being disparities under environmental policies, making environmental justice considerations central to evaluating the distributional impacts of the green transition (Banzhaf et al., 2019; Hsiang et al., 2019; Luo et al., 2025). We therefore examine heterogeneity across a broad spectrum of community characteristics, including income, urbanization, healthcare resources, education, and age structure, to rigorously test for environmental inequality.

The results reveal a strongly regressive pattern across all dimensions. In Column (1), while EV penetration increases NO_2 concentrations by 0.27 on average, the effect is amplified by 0.82 in low-income cities, implying that plants located in poorer areas experience nearly

Table 8: Mechanisms: Decomposing EV Effects With and Without Grid Transmission

	(1)	(2)	(3)
	Excluding Own City		Only Own City
	NO_2 (10 km)	NO_2 (20 km)	NO_2 (10 km)
EV penetration	0.3209***	0.3344***	0.1604**
	(0.1127)	(0.1080)	(0.0696)
Wind speed	1.0663	1.0743	-0.4901
	(5.1317)	(4.8826)	(4.3753)
Pressure	0.2583	0.2788	0.2065
	(0.7155)	(0.6857)	(0.6648)
Temperature	0.0006	0.0003	-0.0006
	(0.0011)	(0.0010)	(0.0009)
Humidity	-0.0136	0.0025	-0.0295
	(0.0403)	(0.0382)	(0.0307)
Constant	4.5014***	4.1674***	4.2115***
	(0.2205)	(0.2065)	(0.1811)
Plant FE	Yes	Yes	Yes
Year-month FE	Yes	Yes	Yes
Observations	192,925	193,798	250,788
R^2	0.7516	0.7514	0.7602

Notes: The dependent variables are NO_2 concentrations measured within 10 km of each plant in Columns (1) and (3) and within 20 km in Column (2). Columns (1) and (2) use EV penetration measured at the province level, excluding the plant's own city, while Column (3) uses city-level EV penetration. All regressions include plant fixed effects, year-month fixed effects, and weather controls. Standard errors in parentheses are clustered at the city level. *, **, and *** denote significance at the 10%, 5%, and 1% levels, respectively.

four times larger pollution increases. Column (2) shows that less urbanized, more rural cities also face significantly higher exposure, with an interaction effect of 0.40. Column (3) indicates that the pollution response is substantially larger in cities with healthcare shortages, where the interaction coefficient reaches 0.77, precisely in locations where populations are least able to mitigate or absorb pollution-related health risks.

Columns (4) through (6) extend the analysis to additional dimensions of disadvantage. Pollution increases are disproportionately concentrated in communities with lower educational attainment. The interaction coefficients for populations with no schooling in Column (4) and high illiteracy rates in Column (5) are 0.82 and 0.79, respectively, indicating that the environmental costs of power generation are systematically shifted toward less educated populations. Column (6) further shows a large positive interaction of 0.85 with the elderly population share. Given the greater physiological susceptibility of older adults to NO_2 exposure, this result suggests that the displaced pollution burden falls not only on economically disadvantaged groups but also on biologically vulnerable populations.

Overall, these estimates underscore a multidimensional environmental injustice embedded in the current transition. While EV adoption reduces pollution in vehicle-dense urban

Table 9: Heterogeneity Analysis on Environmental Justice

	(1)	(2)	(3)	(4)	(5)	(6)
		Rural	Healthcare	Low Education		Elderly
	Poverty	Areas	Shortage	No Schooling	Illiteracy	Population
EV penetration	0.2737**	0.3235**	0.1795	0.2150*	0.2440**	0.1980
	(0.1261)	(0.1299)	(0.1380)	(0.1150)	(0.1210)	(0.1320)
EV penetration×Poverty	0.8202***					
	(0.2164)					
EV penetration×Rural		0.3961*				
		(0.2294)				
EV penetration×HealthShort			0.7698***			
			(0.2046)			
EV penetration×No Schooling				0.8150***		
				(0.1980)		
EV penetration×Illiteracy					0.7850***	
					(0.2010)	
EV penetration×Elderly						0.8520***
						(0.2110)
Constant	4.4671***	4.4668***	4.4742***	4.4580***	4.4610***	4.4650***
	(0.1993)	(0.1992)	(0.1992)	(0.1985)	(0.1988)	(0.1990)
Weather controls	Yes	Yes	Yes	Yes	Yes	Yes
Plant FE	Yes	Yes	Yes	Yes	Yes	Yes
Year-month FE	Yes	Yes	Yes	Yes	Yes	Yes
Observations	225,532	225,532	225,532	225,532	225,532	225,532
R^2	0.766	0.766	0.766	0.767	0.767	0.766

Notes: *Poverty* and *Rural* identify cities in the bottom 25th percentile of GDP per capita and urbanization rate. *No Schooling* and *Illiteracy* measure the share of the population aged 6+ with no formal education and aged 15+ who are illiterate. *Elderly Population* captures the share aged 65+. Indicator variables in columns (4)–(6) equal one for cities in the top 25th percentile of each distribution. Data for columns (4)–(6) come from the 2020 Population Census. Standard errors in parentheses are clustered at the city level. *, **, and *** denote significance at the 10%, 5%, and 1% levels, respectively.

centers and primarily benefits wealthier populations, the associated upstream emissions are disproportionately borne by vulnerable communities, including low-income, rural, medically underserved, less educated, and elderly populations. This asymmetry suggests that without complementary place-based policies, the green transition risks exacerbating existing inequalities by decoupling the global benefits of decarbonization from the localized environmental costs borne by disadvantaged communities.

Thus, the environmental consequences of transportation electrification are unevenly distributed. EV adoption reallocates pollution toward communities that are poorer, more rural, medically underserved, older, and less educated, and these disparities operate both within cities and across cities through the electricity transmission network. The results underscore that achieving an equitable green transition requires policies that align EV promotion with grid decarbonization and targeted protections for vulnerable populations.

8.3 Policy Design: Grid Decarbonization and EV Adoption

We use regional heterogeneity in the estimated EV effects, together with regional electricity generation structures, to assess when electrification policies generate unintended spatial and distributional consequences.

We classify China into seven regions and estimate region-specific effects that vary systematically with generation mix.[17] Table 10 shows the estimated effect of EV penetration on NO_2 concentrations near power plants is positive and statistically significant in several regions, including the Northeast and Northwest. The magnitude and significance of these effects vary systematically with the underlying generation mix rather than with aggregate EV adoption alone. The regions showing statistically significant effects are those with a higher share of coal-fired power plants in installed capacity, as Figure 7 shows. This pattern is difficult to reconcile with a pure demand-reduction narrative and instead points to a spatial reallocation of emissions: electrification reduces tailpipe pollution in consuming cities while increasing emissions at coal-fired plants supplying the additional electricity load. Importantly, economic growth and urbanization in these regions stagnated over much of the study period, yet the estimated effects remain statistically significant, making it unlikely that the results are driven by concurrent economic expansion or other local economic activity.

By contrast, regions with a larger share of hydropower or cleaner generation exhibit weaker or statistically insignificant effects. In the Southwest, where hydropower constitutes the majority of generation capacity throughout the period, the estimated coefficient on EV penetration is smaller and imprecisely estimated. Similarly, in Central China, where coal dependence is lower and the generation mix is more diversified, the relationship between EV adoption and power-plant-level NO_2 is muted.

These findings carry important implications for policy design. They caution against evaluating green transition policies solely based on aggregate emissions reductions or accounting-based compliance metrics. For policymakers, this means the EV adoption can generate a pronounced smokestack-side response when grid decarbonization lags behind electrification. When electrification proceeds faster than grid decarbonization, policies that appear successful at the national level can exacerbate environmental inequality across regions. This risk is particularly acute under non-location-based mechanisms such as renewable energy certificates, which decouple electricity consumption from the physical location of generation and local pollution damages.

The policy implication is not to slow EV adoption, but to better align it with the spatial structure of electricity supply. First, EV promotion should be explicitly coordinated with

[17] Table A.10 shows the detailed classification of provinces for each region.

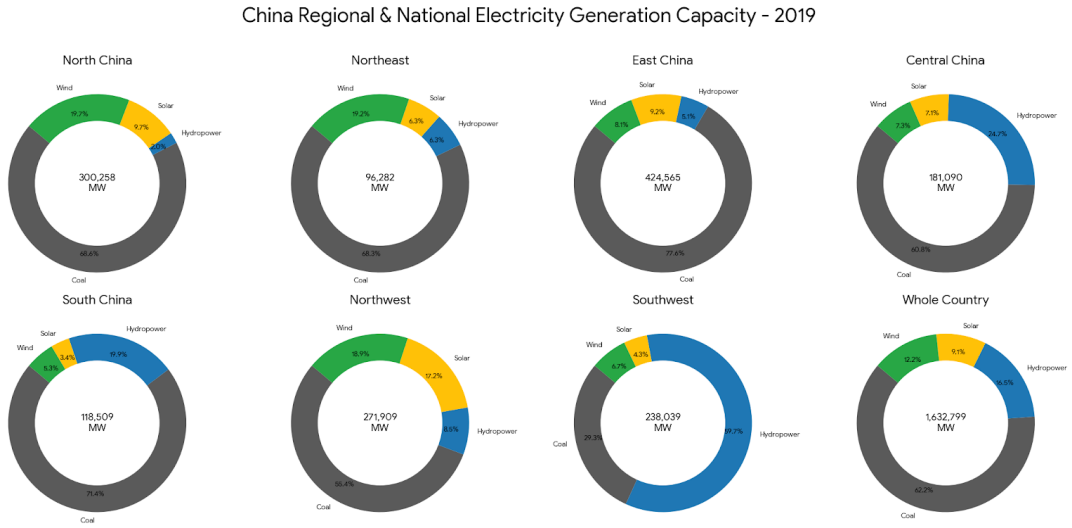
Table 10: Regional Heterogeneity: EV Adoption and NO_2 near Power Plants

	(1) North	(2) Northeast	(3) East	(4) Central	(5) South	(6) Northwest	(7) Southwest
EV penetration	0.3719	0.5345*	0.3428*	0.1209	0.9533**	0.6958*	0.4699
	(0.3303)	(0.2990)	(0.2000)	(0.3079)	(0.3899)	(0.3626)	(0.4737)
Wind speed	-9.0893	-2.6535	0.8639	-19.6433	-17.3178	11.4957	-20.0473
	(16.2367)	(20.1481)	(11.0473)	(24.7584)	(20.3619)	(15.7303)	(19.6523)
Pressure	-4.1353	-1.2233	1.6144	-1.5729	-6.4328	-5.4467	3.8668
	(2.6903)	(7.5512)	(5.3617)	(6.7449)	(9.2306)	(3.2317)	(2.8208)
Temperature	0.0056	0.0001	-0.0053	0.0005	0.0115	0.0026	-0.0055
	(0.0053)	(0.0085)	(0.0039)	(0.0062)	(0.0073)	(0.0053)	(0.0047)
Humidity	0.0641	-0.1556	0.0003	-0.1177	-0.1693	-0.0447	-0.2211
	(0.1754)	(0.2156)	(0.1000)	(0.1322)	(0.2906)	(0.1004)	(0.1718)
Constant	5.7393***	4.5966***	3.2338***	4.7518***	7.0506***	5.1898***	3.2566***
	(1.1241)	(1.2790)	(0.8249)	(1.5706)	(2.0157)	(1.2174)	(0.9832)
Plant FE	Yes	Yes	Yes	Yes	Yes	Yes	Yes
Year-month FE	Yes	Yes	Yes	Yes	Yes	Yes	Yes
Observations	33,555	35,822	80,378	29,213	23,612	22,624	24,373
R^2	0.795	0.790	0.770	0.801	0.812	0.809	0.806

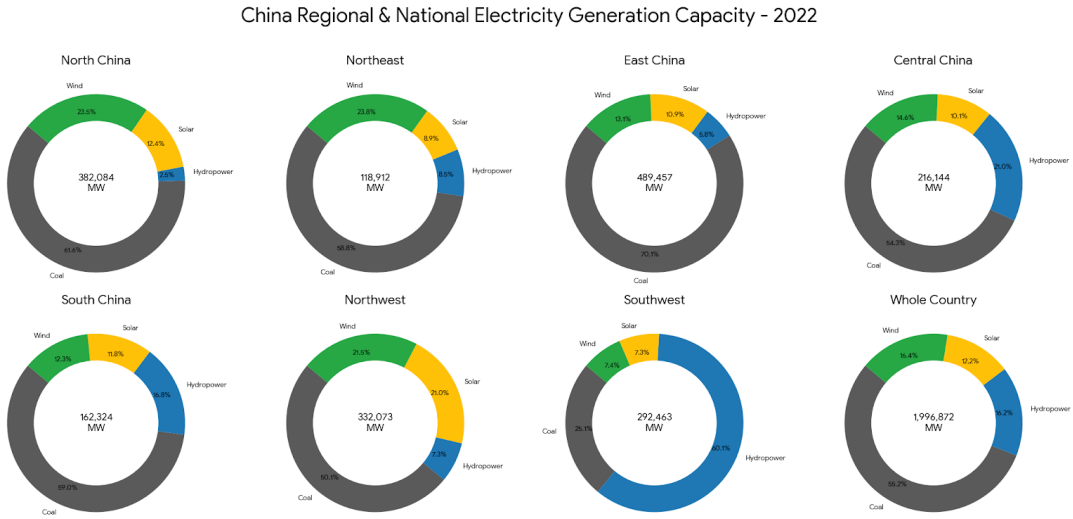
Notes: Each column reports estimates from a separate regression for the indicated region. All regressions include plant fixed effects, year-month fixed effects, and weather controls. Standard errors in parentheses are clustered at the city level. *, **, and *** denote significance at the 10%, 5%, and 1% levels, respectively.

grid-side decarbonization in regions that serve as marginal suppliers, including accelerated coal retirements and binding constraints on high-emitting units. Second, compliance frameworks should move beyond national or average grid shares and instead incorporate location-based or marginal emissions metrics. A kilowatt-hour is not uniformly clean across space; policies that abstract from this heterogeneity risk displacing pollution rather than reducing it. Third, demand-side design warrants greater attention. Because EV charging is often temporally clustered, time-of-use pricing, managed charging, and targeted clean-charging programs can reduce reliance on coal-intensive marginal dispatch. Finally, distributional consequences must be made explicit. If cleaner urban air is achieved in part through higher exposure in power-generating regions, environmental justice cannot remain an implicit objective. Monitoring, disclosure, and compensatory investments should therefore prioritize communities located near thermal power plants.

These dynamics are unlikely to be unique to China. Any rapid electrification pathway that expands electricity demand faster than clean generation, and relies heavily on non-local compliance mechanisms, faces a similar risk: visible improvements in urban air quality accompanied by less visible, but no less consequential, increases in pollution exposure elsewhere. Recognizing and addressing this tradeoff is essential for designing a green transition that is both effective and equitable.



(a) Regional Electricity Generation Capacity Structure (2019)



(b) Regional Electricity Generation Capacity Structure (2022)

Figure 7: Evolution of China's Electricity Generation Capacity Structure (2019–2022)

Notes: Capacity is measured in megawatts (MW) and includes coal, hydropower, solar, and wind plants from Global Energy Monitor. The "Whole Country" series aggregates operating capacity across all provinces, with regions defined by standard Chinese geographical divisions. From 2019 to 2022, China's power system diversified rapidly: East China combined a large coal base with fast growth in wind and solar; the Northwest emerged as a renewable hub with wind and solar capacity approaching coal; the Northeast experienced a gradual coal–wind transition; and South China expanded solar while maintaining coal for grid stability.

8.4 Back-of-the-Envelope Cost-Benefit Analysis

Aggregate Health Benefits and Distributional Implications of Vehicle Electrification. Figure 8 and Table A.11 presents a back-of-the-envelope cost-benefit analysis that monetizes the health gains from reducing very low birth weight (VLBW) births through EV adoption.[18] Following the framework of Currie et al. (2022), we estimate the social cost per avoided VLBW birth by aggregating six components: infant mortality, acute medical care, childhood disability, adult income losses, adult disability medical care, and long-term mortality risk.

We focus on VLBW as our primary health endpoint for several reasons. First, recent evidence from Baran et al. (2025) documents that EV adoption substantially improves infant health, with VLBW serving as a sensitive indicator of prenatal air pollution exposure. The well-established dose-response relationship between NO_2 and VLBW in the Chinese context (Zhou et al., 2023), combined with its characterization as a sentinel indicator for acute pollution effects, makes it ideal for quantifying health impacts. Second, the economic burden of VLBW is disproportionately high due to intensive neonatal care requirements and persistent human capital penalties, allowing us to capture the most tangible and economically significant portion of health benefits. Third, our analysis aims to illuminate environmental justice tensions in green transitions: in coal-dependent economies like China, vehicle electrification may displace pollution from urban centers to power-generating regions. By quantifying both urban health benefits and distributional burdens near power plants through a common VLBW framework, we provide a tractable approach for demonstrating that welfare assessments must account for asymmetric outcomes across populations. While this focus provides a credible lower bound for policy evaluation, it necessarily understates total health impacts.

To quantify aggregate benefits, we combine our reduced-form pollution estimates with dose-response relationships from recent epidemiological studies. Specifically, a one-standard-deviation increase in EV adoption (SD = 0.040) reduces urban NO_2 concentrations by 4.87 $\mu g/m^3$ ($\beta = -1.2175$, SE = 0.318). Applying the first-trimester dose-response parameter from Zhou et al. (2023) (RR = 1.131 per 10 $\mu g/m^3$ NO_2), this air quality improvement translates to approximately 5,229 avoided VLBW births annually. As shown in Table A.11, these avoided cases generate an annual welfare gain of $3.04 billion, cumulating to $12.17 billion over 2019–2022.[19] These localized health gains from VLBW reductions alone offset a

[18] Due to the absence of individual-level health data in China, we combine our reduced-form pollution estimates with established dose-response functions from the epidemiological literature to assess the order of magnitude of health benefits and distributional costs associated with vehicle electrification.

[19] In addition to the VLBW-based estimates, we calculate adult mortality benefits as an alternative benchmark. Using our regression coefficient ($\beta = -1.4321$) and current average EV penetration (0.5%), the observed NO_2 reduction of 0.007 $\mu g/m^3$ translates to approximately 900 avoided premature deaths annually

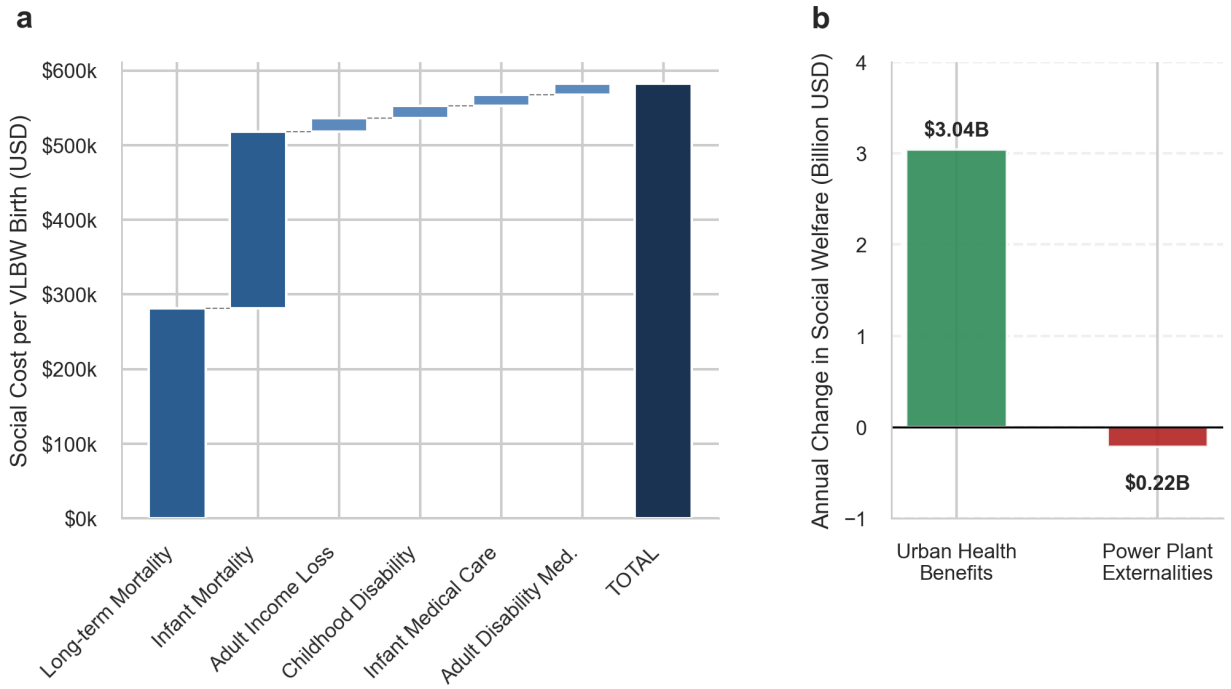


Figure 8: Social Cost Decomposition and Aggregate Welfare Effects of EV Adoption

Notes: This figure reports a back-of-the-envelope welfare calculation based on evidence on very low birth weight (VLBW). Panel A decomposes per-infant social costs using the Value of a Statistical Life (VSL) and medical cost estimates from CHNN (2022) and the National Bureau of Statistics of China; mortality risk accounts for over 85% of total costs. Panel B aggregates these costs to annual welfare effects. Urban benefits reflect an estimated 5,229 avoided VLBW births per year, while power-plant communities incur costs associated with 372 additional births.

substantial portion of fiscal subsidies for EV adoption, highlighting previously unaccounted co-benefits of China's electrification policy.

These estimates represent a *conservative lower bound* of total welfare gains for several reasons. Our calculation focuses exclusively on severe VLBW cases, omitting benefits from: (i) reductions in moderate low birth weight and preterm births; (ii) improvements in respiratory health across age groups; (iii) productivity gains from reduced pollution exposure; and (iv) global climate benefits from carbon abatement. Consequently, the true societal value of EV adoption likely exceeds our VLBW-based estimate by a substantial margin.

Environmental Justice and the Distributive Costs of Pollution Displacement. While our primary analysis confirms substantial aggregate health benefits from electric vehi-

(applying the dose-response parameter of 12.7% mortality reduction per 10 $\mu g/m^3$ NO_2 decrease). Valued at a conservative VSL of \$1.15 million per statistical life, this yields an annual welfare gain of \$1.04 billion from adult mortality reduction alone, corroborating substantial health co-benefits even at early-stage EV adoption.

cle adoption in urban centers, the distributional consequences of this transition merit careful examination. By mapping the pollution plume of EV charging to lower-income power plant communities, we document a green gentrification of air quality, where environmental improvements in wealthy demand centers are partially financed by the health degradation of peripheral supply regions. Populations residing near coal-fired power plants are often socioeconomically vulnerable, making them disproportionately susceptible to environmental hazards (Currie et al., 2015; Banzhaf et al., 2019). Estimating the health costs borne by these communities is therefore essential for assessing the environmental justice implications of China's vehicle electrification strategy.

Supplementary analysis of power-plant-adjacent counties in Panel b of Figure 8 shows that a one-standard-deviation increase in EV adoption (SD = 0.040) is associated with a 1.73 $\mu g/m^3$ increase in local NO_2 concentrations ($\beta = 0.433$, SE = 0.124). This finding confirms that urban air quality improvements partly come at the expense of air quality in electricity-generating regions. Applying the dose-response function from Zhou et al. (2023) and assuming conservatively that 20 percent of the national birth cohort faces exposure to power plant emissions, we estimate this pollution displacement induces approximately 372 additional very low birth weight cases annually among these communities.

Monetizing these adverse outcomes using the VSL-adjusted valuation yields an estimated annual social cost of \$0.22 billion borne by populations near power infrastructure.[20] While this burden represents a distinct cost stream rather than a direct offset to aggregate benefits, it underscores a non-negligible environmental justice concern concentrated among socioeconomically vulnerable communities. These localized health damages highlight that the welfare assessment of vehicle electrification must account for both efficiency gains and distributional equity. Achieving a just transition requires complementary policies such as accelerated grid decarbonization and targeted compensation mechanisms for affected regions.

9 Conclusions

This paper provides the first empirical evidence on the spatial redistribution of air pollution induced by the rapid adoption of electric vehicles in China. By combining high-resolution satellite measures of NO_2, SO_2, and O_3 with ground-station measurements of $PM_{2.5}$, together

[20]We present the aggregate health benefits and distributional burdens separately rather than netting them out due to data source heterogeneity. The urban estimates utilize ground-level monitoring data, whereas power plant estimates rely on satellite-derived pollution concentrations. Consequently, these figures are not strictly comparable numerically and should not be directly summed or compared as proportions. Our primary objective is to demonstrate the substantial aggregate welfare gains from EV adoption while explicitly acknowledging the environmental justice implications, where vulnerable populations near power infrastructure bear distinct additional costs.

with detailed data on coal-fired power plants and city-level EV penetration, we document a clear trade-off. While EV adoption reduces urban air pollution, it increases pollution exposure in communities located near power plants supplying the additional electricity, both within cities and across cities. These results highlight the central role of the electricity grid in mediating the environmental consequences of transportation electrification.

We provide two main policy implications. First, the environmental benefits of EV adoption depend critically on the cleanliness of the electricity grid. In regions where coal remains the marginal source of power, electrification shifts pollution away from urban roadways toward plant-adjacent communities, many of which are economically disadvantaged. This highlights the importance of coordinating EV promotion with grid decarbonization. Second, the uneven distribution of costs and benefits raises concerns about environmental justice. Policies such as stricter emissions standards for power plants, targeted compensation for affected communities, and accelerated investment in clean generation and transmission infrastructure can help mitigate these regressive impacts.

The framework developed in this paper can be applied to other countries undergoing rapid electrification, where fossil fuels remain dominant in power generation. As countries pursue ambitious climate goals, understanding the spatial and distributional dynamics of clean technology adoption becomes increasingly important. This study underscores that effective climate policy must integrate equity considerations alongside efficiency and emissions reduction. Ensuring that the benefits of electrification are broadly shared, while avoiding the concentration of environmental burdens on vulnerable communities, is central to achieving a just and durable green transition.

References

Anderson, Wayne L, Brian S Armour, Eric A Finkelstein, and Joshua M Wiener. 2010. "Estimates of state-level health-care expenditures associated with disability." *Public Health Reports*, 125(1): 44–51.

Archsmith, James, Alissa Kendall, and David Rapson. 2015. "From Cradle to Junkyard: Assessing the Life Cycle Greenhouse Gas Benefits of Electric Vehicles." *Research in Transportation Economics*, 50: 72–90.

Arkolakis, Costas, and Conor Walsh. 2023. "Clean growth." National Bureau of Economic Research.

Arkolakis, Costas, Kenneth T Gillingham, and Seung-Yong Yoo. 2025. "Optimizing Electric Vehicle Infrastructure." *AEA Papers and Proceedings*, 115: 563–567.

Balboni, Clare, and Joseph S Shapiro. 2025. "Spatial environmental economics." In *Handbook of Regional and Urban Economics*. Vol. 6, Chapter 9, 585–652. Elsevier.

Banzhaf, Spencer, Lala Ma, and Christopher Timmins. 2019. "Environmental Justice: The Economics of Race, Place, and Pollution." *Journal of Economic Perspectives*, 33(1): 185–208.

Baran, Cavit, Janet Currie, Bahadir Dursun, and Erdal Tekin. 2025. "Clean rides, healthy lives: The impact of electric vehicle adoption on air quality and infant health." National Bureau of Economic Research.

Barwick, Panle Jia, Hyuk-soo Kwon, and Shanjun Li. 2022. "Attribute-Based Subsidies and Market Power: An Application to Electric Vehicles." *Unpublished working paper*.

Barwick, Panle Jia, Hyuk-soo Kwon, Shanjun Li, and Nahim Bin Zahur. 2024. "Driving Down the Cost: Learning By Doing and Government Policy in the Electric Vehicle Battery Industry." *Working Paper, 2024*.

Bharadwaj, Prashant, Juan Pedro Eberhard, and Christopher A Neilson. 2018. "Health at birth, parental investments, and academic outcomes." *Journal of Labor Economics*, 36(2): 349–394.

Borenstein, Severin, and Lucas W Davis. 2016. "The Distributional Effects of US Clean Energy Tax Credits." *Tax Policy and the Economy*, 30(1): 191–234.

Carril-Caccia, Federico, and Juliette Milgram Baleix. 2024. "Trade, Growth, and the Environment." *Journal of Environmental Economics and Management*, 127: 103038.

China Energy Transformation Programme. 2025. "China Energy Transformation Outlook 2024." China Energy Transformation Programme Technical Report. Accessed: 2025-12-15.

Colmer, Jonathan, Suzy Qin, John Voorheis, and Reed Walker. 2024. "The changing nature of pollution, income, and environmental inequality in the United States." *AEA Papers and Proceedings*, 114: 41–46.

Copeland, Brian R., and M.Scott Taylor. 2004. "Trade, Growth, and the Environment." *Journal of Economic Literature*, 42(1): 7–71.

Currie, Janet, John Voorheis, and Reed Walker. 2023. "What caused racial disparities in particulate exposure to fall? New evidence from the Clean Air Act and satellite-based measures of air quality." *American Economic Review*, 113(1): 71–97.

Currie, Janet, Lucas Davis, Michael Greenstone, and Reed Walker. 2015. "Environmental Health Risks and Housing Values: Evidence from 1,600 Toxic Plant Openings and Closings." *American Economic Review*, 105(2): 678–709.

Currie, Janet, Michael Mueller-Smith, and Maya Rossin-Slater. 2022. "Violence While in Utero: The Impact of Assaults during Pregnancy on Birth Outcomes." *Review of Economics and Statistics*, 104(3): 525–540.

Cutler, David M, and Ellen Meara. 2000. "The technology of birth: Is it worth it?" In *Frontiers in Health Policy Research, Volume 3*. 33–68. MIT Press.

Davis, Lucas W. 2011. "The effect of power plants on local housing values and rents." *Review of Economics and Statistics*, 93(4): 1391–1402.

Domínguez-Iino, Tomás. 2023. "Spatial economics and environmental policies." *Handbook of Labor, Human Resources and Population Economics*, 1–16.

Fang, Hanming, Ming Li, Long Wang, and Zoe Yang. 2025. "High-Speed Rail and China's Electric Vehicle Adoption Miracle." National Bureau of Economic Research.

Fan, Maoyong, Guojun He, and Maigeng Zhou. 2020. "The winter choke: Coal-fired heating, air pollution, and mortality in China." *Journal of Health Economics*, 71: 102316.

Fowlie, Meredith, Mar Reguant, and Stephen P Ryan. 2016. "Market-Based Emissions Regulation and Industry Dynamics." *Journal of Political Economy*, 124(1): 249–302.

Fowlie, Meredith, Reed Walker, and David Wooley. 2020. "Climate policy, environmental justice, and local air pollution." Brookings Institution Economic Studies at Brookings.

Gao, Zhengye, and Li Zhao. 2025. "Health impacts of cross-regional transmission infrastructure: Evidence from China's ultra-high voltage projects." *Energy Economics*, 148: 108669.

García-Muros, Xaquín, Jennifer Morris, and Sergey Paltsev. 2022. "Toward a just energy transition: A distributional analysis of low-carbon policies in the USA." *Energy Economics*, 105: 105769.

Gillingham, Kenneth T, Marten Ovaere, and Stephanie M Weber. 2025. "Carbon policy and the emissions implications of electric vehicles." *Journal of the Association of Environmental and Resource Economists*, 12(2): 313–352.

Graff Zivin, Joshua S., Matthew J. Kotchen, and Erin T. Mansur. 2014. "Spatial and Temporal Heterogeneity of Marginal Emissions: Implications for Electric Cars and Other Electricity-Shifting Policies." *Journal of Economic Behavior & Organization*, 107: 248–268.

Greenstone, Michael, Guojun He, Shanjun Li, and Eric Zou. 2021. "China's War on Pollution: Evidence from the First 5 Years." *Review of Environmental Economics and Policy*, 15(2): 281–299.

Gutman, Richard, PP Marchenko, and RD Dunlop. 1979. "Analytical development of loadability characteristics for EHV and UHV transmission lines." *IEEE Transactions on Power Apparatus and Systems*, 98(2): 606–617.

Hack, Maureen, Daniel J Flannery, Mark Schluchter, Lydia Cartar, Elaine Borawski, and Nancy Klein. 2002. "Outcomes in young adulthood for very-low-birthweight infants." *New England Journal of Medicine*, 346(3): 149–157.

Hanig, Lily, Corey D Harper, Destenie Nock, and Jeremy J Michalek. 2025. "Driving the grid forward: How electric vehicle adoption shapes power system infrastructure and emissions." *Proceedings of the National Academy of Sciences*, 122(37): e2420609122.

Harvey, Fiona. 2024. "China adds new clean power equivalent to UK's entire electricity output." *The Guardian*. Accessed: 2025-12-15.

Hernandez-Cortes, Danae, and Kyle C Meng. 2023. "Do Environmental Markets Cause Environmental Injustice? Evidence from California's Cap-and-Trade." *Journal of Public Economics*, 217: 104786.

Holladay, J Scott, and Jacob LaRiviere. 2017. "The impact of cheap natural gas on marginal emissions from electricity generation and implications for energy policy." *Journal of Environmental Economics and Management*, 85: 205–227.

Holland, Stephen P, Erin T Mansur, and Andrew J Yates. 2021. "The electric vehicle transition and the economics of banning gasoline vehicles." *American Economic Journal: Economic Policy*, 13(3): 316–344.

Holland, Stephen P, Erin T Mansur, Nicholas Z Muller, and Andrew J Yates. 2016. "Are there environmental benefits from driving electric vehicles? The importance of local factors." *American Economic Review*, 106(12): 3700–3729.

Holland, Stephen P, Erin T Mansur, Nicholas Z Muller, and Andrew J Yates. 2019. "Distributional effects of air pollution from electric vehicle adoption." *Journal of the Association of Environmental and Resource Economists*, 6(S1): S65–S94.

Hsiang, Solomon, Paulina Oliva, and Reed Walker. 2019. "The distribution of environmental damages." *Review of Environmental Economics and Policy*, 13(1): 83–103.

Huang, I-Chan, Joy L Lee, Pavinarmatha Ketheeswaran, Conor M Jones, Dennis A Revicki, and Albert W Wu. 2017. "Does personality affect health-related quality of life? A systematic review." *PloS one*, 12(3): e0173806.

Jacqz, Irene, and Sarah Johnston. 2024. "Electric vehicle subsidies and urban air pollution disparities." *Journal of the Association of Environmental and Resource Economists*, 11(S1): S41–S69.

Jia, Wentao, Chunbo Ma, XIiao Wang, and Rui Xie. 2025. "Intra-firm pollution leakage and redistribution of pollution exposure: Evidence from coal-regulated plants in China." *Journal of Environmental Economics and Management*, 133: 103205.

Jia, Zhijie, Shiyan Wen, and Yao Wang. 2023. "Power coming from the sky: Economic benefits of inter-regional power transmission in China." *Energy Economics*, 119: 106544.

Li, Jing. 2019. "Compatibility and investment in the US electric vehicle market." *Unpublished manuscript, MIT*.

Lin, Boqiang, and Wei Wu. 2021. "The impact of electric vehicle penetration: A recursive dynamic CGE analysis of China." *Energy Economics*, 94: 105086.

Li, Ruiyao, Rui Wang, Haoran Li, Jin Li, Shihui Zhang, Mengzhen Zhao, Can Wang, and Wenjia Cai. 2025. "Multidimensional inequality embedded in the gains and losses from China's coal phasedown." *Nexus*, 2(4).

Li, Shanjun, Lang Tong, Jianwei Xing, and Yiyi Zhou. 2017. "The market for electric vehicles: indirect network effects and policy design." *Journal of the Association of Environmental and Resource Economists*, 4(1): 89–133.

Li, Shanjun, Xianglei Zhu, Yiding Ma, Fan Zhang, and Hui Zhou. 2022. "The role of government in the market for electric vehicles: Evidence from China." *Journal of Policy Analysis and Management*, 41(2): 450–485.

Liu, Youming, Shanjun Li, and Caixia Shen. 2020*a*. "The dynamic efficiency in resource allocation: Evidence from vehicle license lotteries in Beijing." National Bureau of Economic Research.

Liu, Zhu, Philippe Ciais, Zhu Deng, Ruixue Lei, Steven J Davis, Sha Feng, Bo Zheng, Duo Cui, Xinyu Dou, Biqing Zhu, et al. 2020*b*. "Near-real-time monitoring of global CO2 emissions reveals the effects of the COVID-19 pandemic." *Nature Communications*, 11(1): 5172.

Luo, Zhonghui, Lala Ma, Rui Xie, and Ran Song. 2025. "A spatially differentiated water pollution policy leads to economic and health inequity." *Proceedings of the National Academy of Sciences*, 122(39): e2421404122.

Lyapustin, Alexei, Yujie Wang, Sergey Korkin, and Dong Huang. 2018. "MODIS collection 6 MAIAC algorithm." *Atmospheric Measurement Techniques*, 11(10): 5741–5765.

Ma, Lala. 2020. "Mapping the clean air haves and have-nots." *Science*, 369(6503): 503–504.

Matthews, TJ, Marian F MacDorman, and Marie E Thoma. 2015. "Infant Mortality Statistics From the 2013 Period Linked Birth/Infant Death Data Set." *National vital statistics reports: from the Centers for Disease Control and Prevention, National Center for Health Statistics, National Vital Statistics System*, 64(9): 1–30.

Meckling, Jonas. 2025. "The geoeconomic turn in decarbonization." *Nature*, 645(8082): 869–876.

Mei, Yingdan, Jixiang Qiu, Wendong Zhang, Sookti Chaudhary, and Pengfei Liu. 2025. "Carbon markets promote environmental justice in China." *Nature Communications*.

Michalek, Jeremy J, Mikhail Chester, Paulina Jaramillo, Constantine Samaras, Ching-Shin Norman Shiau, and Lester B Lave. 2011. "Valuation of plug-in vehicle life-cycle air emissions and oil displacement benefits." *Proceedings of the National Academy of Sciences*, 108(40): 16554–16558.

Morehouse, John, and Edward Rubin. 2021. "Downwind and out: The strategic dispersion of power plants and their pollution." *Available at SSRN 3915247*.

Muehlegger, Erich, and David S Rapson. 2022. "Subsidizing Mass Adoption of Electric Vehicles: Quasi-Experimental Evidence from California." *Journal of Public Economics*, 210: 104632.

Nehiba, Cody. 2024. "Electric vehicle usage, pollution damages, and the electricity price elasticity of driving." *Journal of Environmental Economics and Management*, 124: 102915.

Pizer, William A, and Steven Sexton. 2019. "The distributional impacts of energy taxes." *Review of Environmental Economics and Policy*.

Qin, Qi, and Christine Shearer. 2025. "Coal Is Losing Ground, but Not Letting Go: Structural Inertia and the Struggle to Shift Coal's Role in China's Power System." *Centre for Research on Energy and Clean Air and Global Energy Monitor*.

Ren, Shenggang, Li Zhao, Peng Zhang, and Caiquan Bai. 2026. "Pollution Reduction Effects of New Transregional Power Transmission Systems: Evidence from Ultra-High-Voltage Projects of China." *Journal of Development Economics*, 179: 103641.

Schöngart, Sarah, Zebedee Nicholls, Roman Hoffmann, et al. 2025. "High-income groups disproportionately contribute to climate extremes worldwide." *Nature Climate Change*, 15(1): 627–633.

Shapiro, Joseph S, and Reed Walker. 2018. "Why is pollution from US manufacturing declining? The roles of environmental regulation, productivity, and trade." *American Economic Review*, 108(12): 3814–3854.

Shu, Li, Chunhua Wang, and Wei Wang. 2025. "Vehicle exhaust standards and urban air quality in China." *Journal of Development Economics*, 172: 103387.

Simshauser, Paul, and Phillip Wild. 2025. "Rooftop solar PV, coal plant inflexibility and the minimum load problem." *The Energy Journal*, 46(1): 93–118.

Sioshansi, Ramteen, and Paul Denholm. 2010. "The value of plug-in hybrid electric vehicles as grid resources." *The Energy Journal*, 31(3): 1–24.

The Economic Times. 2024. "China accounted for 80% of global EV sales growth in 2024: IEA report." *https://economictimes.indiatimes.com/industry/renewables/china-accounted-for-80-of-global-ev-sales-growth-in-2024-iea-report/articleshow/116650897.cms?from=mdr*, Accessed: 2025-12-05.

Wang, Hui, Yunyun Zhang, Weifen Lin, and Wendong Wei. 2023. "Transregional electricity transmission and carbon emissions: evidence from ultra-high voltage transmission projects in China." *Energy Economics*, 123: 106751.

Xing, Jianwei, Benjamin Leard, and Shanjun Li. 2021. "What does an electric vehicle replace?" *Journal of Environmental Economics and Management*, 107: 102432.

Xinhua News Agency. 2025. "Shenzhen Promotes Green Electricity Use for Electric Vehicle Charging." *https://www.xinhuanet.com/20250815/4548eb3977044aa4a74466cd28c18a29/c.html*, Accessed August 2025.

Yu, Chengcheng, Quan Yuan, Anne Goodchild, Wentao Dong, Travis Fried, Haocheng Lin, Yeke Zou, Chao Yang, Yougeng Lu, Qianyao Duan, and Zhengtao Qin. 2026. "Increasing nationwide disparities in road freight emissions across cities." *Nature Cities*, 3(1): 28–37.

Zhang, Xiaoli, Xueqin Cui, Bo Li, Patricia Hidalgo-Gonzalez, Daniel M Kammen, Ji Zou, and Ke Wang. 2022. "Immediate actions on coal phaseout enable a just low-carbon transition in China's power sector." *Applied Energy*, 308: 118401.

Zhou, Wenjuan, Xian Ming, Yiqiong Yang, Yu Hu, Zhoupeng He, Hongyan Chen, Yan Li, Jian Cheng, and Xiaojun Zhou. 2023. "Associations between maternal exposure to ambient air pollution and very low birth weight: A birth cohort study in Chongqing, China." *Frontiers in Public Health*, 11: 1123594.

Zhuge, Chengxiang, Binru Wei, Chunfu Shao, Yuli Shan, and Chunjiao Dong. 2020. "The role of the license plate lottery policy in the adoption of Electric Vehicles: A case study of Beijing." *Energy Policy*, 139: 111328.

Online Appendix for

"Geospatial Inequality in the Green Transition: Pollution Redistribution from Electric Vehicles"

Appendix Contents

1. Additional Figures and Tables A2
2. Wind-Adjustment Pollution A15
3. Unit Conversion of Air Pollution Measures A15
4. Conceptual Model of Pollution Redistribution A16
5. Electricity Dispatch and Inter-city Transmission A20

A Additional Figures and Tables

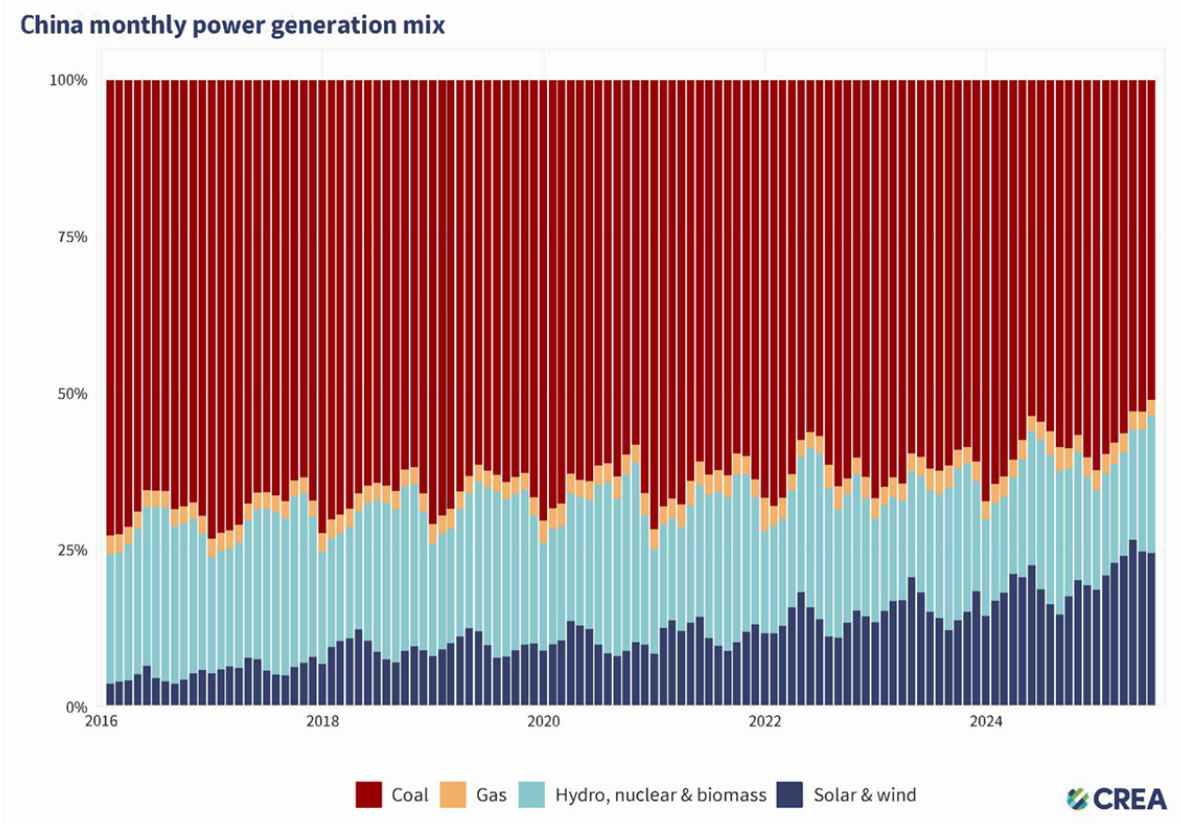


Figure 2 – China monthly power generation mix 2016-H1 2025

Figure A.1: Structural Persistence of Coal in China's Power System

Notes: The figure illustrates the continued dominance of coal-fired power generation in China despite rapid growth in renewable capacity. It highlights the role of structural inertia in the power system, whereby coal remains the primary marginal source of electricity generation, especially during demand surges.
Source: Coal is Losing Ground but Not Letting Go: Structural Inertia and the Struggle to Shift Coal's Role in China's Power System, Centre for Research on Energy and Clean Air (CREA) and Global Energy Monitor (GEM), 2025.



Figure A.2: Empirical Designs for Estimating the Pollution Gradient Around Power Plants

Notes: Panel 1 illustrates the spatial Difference-in-Differences design, in which areas within 0–10 km of a coal-fired power plant serve as the treatment zone, and areas 20-50 km away serve as the control zone. The 10-20 km buffer zone provides an intermediate exposure band. Panel 2 shows the expected regression relationship: increases in EV adoption raise marginal electricity demand, causing plants to ramp up generation and intensifying pollution exposure in near-plant areas relative to farther locations. Panel 3 presents a robustness test based on wind direction. Because emissions are transported downwind, only downwind locations should exhibit pollution responses to EV-induced generation shocks, while upwind and crosswind locations should not. Together, these panels summarize the empirical logic behind the smokestack effect and the spatial gradient identification strategy.

Table A.1: Robustness Check: Effects of EV Adoption on Other Pollutants

	SO_2 (10 km)	O_3 (5 km)
	(1)	(2)
EV penetration	2.1120*	0.0065***
	(1.1270)	(0.0004)
Wind speed	-77.8725	0.0111
	(48.9228)	(0.0148)
Pressure	3.2092	-0.0011
	(6.9147)	(0.0022)
Temperature	-0.0179	0.0000
	(0.0114)	(0.0000)
Humidity	0.2513	0.0000
	(0.3384)	(0.0001)
Constant	16.6367***	0.1383***
	(2.2683)	(0.0005)
Plant FE	Yes	Yes
Year-month FE	Yes	Yes
Observations	216,780	253,297
R^2	0.4985	0.8136

Notes: Dependent variables are SO_2 concentrations within 10 km of plants (Column 1) and O_3 concentrations within 5 km (Column 2). All regressions include plant and year-month fixed effects and weather controls. Standard errors are reported in parentheses and are clustered at the city level. *, **, and *** indicate significance at the 10%, 5%, and 1% levels, respectively.

Table A.2: Other Robustness Checks

	(1) Log EV Pen.	(2) Long Diff.	(3) Plant Clust.	(4) Province Clust.
ln(EV penetration)	0.4743***			
	(0.1274)			
Δ(EV penetration)		0.2503**		
		(0.1027)		
EV penetration			0.4325***	0.4383***
			(0.1075)	(0.0787)
Wind speed	-0.2225	-4.9690	-0.2260	-0.4080
	(4.4085)	(4.9826)	(4.4145)	(4.6663)
Pressure	0.2321	0.8047	0.2320	0.3032
	(0.6730)	(0.7651)	(0.6747)	(0.6232)
Temperature	-0.0005	-0.0015	-0.0005	-0.0005
	(0.0009)	(0.0010)	(0.0009)	(0.0008)
Humidity	-0.0290	-0.0299	-0.0290	-0.0304
	(0.0307)	(0.0353)	(0.0308)	(0.0320)
Constant	4.2323***	-0.2802	4.2322***	4.2204***
	(0.1816)	(0.2195)	(0.1914)	(0.1632)
Plant FE	Yes	Yes	Yes	Yes
Year-month FE	Yes	Yes	Yes	Yes
Observations	250,838	187,122	250,838	250,452
R^2	0.7600	0.2895	0.7600	0.7599

Notes: Column (1) uses the logarithm of EV penetration. Column (2) estimates a long-difference specification using year-over-year changes in EV penetration. Columns (3) and (4) replicate the baseline specification with alternative clustering levels at the plant level and province level, respectively. All regressions include plant and year-month fixed effects and weather controls. Standard errors are reported in parentheses and are clustered at the city level. *, **, and *** denote significance at the 10%, 5%, and 1% levels.

Table A.3: Provincial Winter Heating Policies in China

Province Name	Heating Rule	Heating Start	Heating End
Beijing	Nov–Mar	11–15	03–15
Tianjin	Nov–Mar	11–15	03–15
Hebei	Nov–Mar	11–15	03–15
Shanxi	Nov–Mar	11–01	03–31
Inner Mongolia	Oct–Apr	10–15	04–15
Liaoning	Nov–Mar	11–01	03–31
Jilin	Oct–Apr	10–20	04–15
Heilongjiang	Oct–Apr	10–20	04–20
Shandong	Nov–Mar	11–15	03–15
Henan	Nov–Mar	11–15	03–15
Shaanxi	Nov–Mar	11–15	03–15
Gansu	Nov–Mar	11–01	03–31
Qinghai	Oct–Apr	10–15	04–15
Ningxia	Nov–Mar	11–01	03–31
Xinjiang	Oct–Apr	10–10	04–10

Notes: The table reports official provincial winter heating policies in China, including heating duration and start/end dates. These policies are used to construct the winter heating dummy in the empirical analysis.

Table A.4: EV Adoption and Air Pollution Using City-Level Monitoring Station Data

VARIABLES	(1) ln(AQI)	(2) ln(NO_2)	(3) ln($PM_{2.5}$)	(4) ln(PM_{10})	(5) ln(O_3)
EV ratio	−0.1136***	−0.1724***	−0.1105***	−0.1508***	−0.0731*
	(0.0301)	(0.0465)	(0.0367)	(0.0385)	(0.0395)
Constant	4.1835***	3.2152***	3.8018***	4.1915***	3.4690***
	(0.0552)	(0.0026)	(0.0730)	(0.0631)	(0.0767)
Weather controls	Yes	Yes	Yes	Yes	Yes
City by Year FE	Yes	Yes	Yes	Yes	Yes
Station by Year FE	Yes	Yes	Yes	Yes	Yes
Province by Year-month FE	Yes	Yes	Yes	Yes	Yes
Observations	128,192	129,881	128,158	128,188	128,206
R^2	0.9359	0.9149	0.9310	0.9392	0.9004

Notes: This table reports robustness check estimates using air quality monitoring station data from 2016 to 2022. The dependent variables are logarithmic concentrations of AQI and major pollutants measured at monitoring stations. All specifications include weather controls, city-by-year fixed effects, station-by-year fixed effects, and province-by-year-month fixed effects. Standard errors are reported in parentheses and are clustered at the city level. *, **, and *** denote statistical significance at the 10%, 5%, and 1% levels, respectively.

Table A.5: EV Adoption and Air Pollution: Monitoring Station Evidence (2016-2022)

	10 km radius			5 km radius		
	(1)	(2)	(3)	(4)	(5)	(6)
VARIABLES	$\ln(NO_2)$	$\ln(SO_2)$	$\ln(PM_{2.5})$	$\ln(NO_2)$	$\ln(SO_2)$	$\ln(PM_{2.5})$
EV ratio	0.1087*	0.1796*	0.1601**	0.1871**	0.1581	0.2913***
	(0.0645)	(0.1079)	(0.0807)	(0.0723)	(0.1217)	(0.0901)
Constant	3.7286***	2.8009***	4.1074***	3.6377***	2.7885***	3.9700***
	(0.0476)	(0.0791)	(0.0729)	(0.0580)	(0.0788)	(0.0708)
Weather controls	Yes	Yes	Yes	Yes	Yes	Yes
City by Year FE	Yes	Yes	Yes	Yes	Yes	Yes
Station by Year FE	Yes	Yes	Yes	Yes	Yes	Yes
Year-month FE	Yes	Yes	Yes	Yes	Yes	Yes
Observations	46,985	46,984	46,978	23,212	23,212	23,209
R^2	0.8782	0.8312	0.8645	0.8783	0.8327	0.8622

Notes: This table reports the impact of EV adoption on air pollution using monitoring station data from 2016 to 2022. The dependent variables are the natural logarithms of pollutant concentrations. Columns (1)–(3) report results for air quality monitors that have at least one power plant within a 10 km radius. Columns (4)–(6) report results for monitors with at least one power plant within a 5 km radius. All specifications include weather controls, city by year fixed effects, station by year fixed effects, and year-month fixed effects. Standard errors are reported in parentheses and are clustered at the city level. *, **, and *** denote significance at the 10%, 5%, and 1% levels, respectively.

Table A.6: EV Adoption and Air Pollution by Number of Power Plants within 5 km

VARIABLES	(1) Plants ≥ 3	(2) Plants ≥ 2	(3) Plants ≥ 1	(4) & (5) Plants $= 0$	
EV ratio	0.2091*	0.1869**	0.1871**	-0.0180	-0.1189***
	(0.1075)	(0.0787)	(0.0723)	(0.0539)	(0.0457)
Constant	3.7374***	3.6835***	3.6377***	3.7055***	3.4303***
	(0.0784)	(0.0545)	(0.0580)	(0.0393)	(0.0589)
Weather controls	Yes	Yes	Yes	Yes	Yes
City by Year FE	Yes	Yes	Yes	Yes	Yes
Station by Year FE	Yes	Yes	Yes	Yes	Yes
Year-month FE	Yes	Yes	Yes	Yes	
Province by Year-month FE					Yes
Observations	11,294	20,631	23,212	71,240	71,240
R^2	0.8757	0.8792	0.8783	0.8907	0.9239

Notes: This table presents the effect of EV adoption on NO_2 concentrations across monitoring stations with varying proximity to coal-fired power plants, using data from 2016 to 2022. The unit of observation is monitor-year-month. Columns (1)–(3) present results for stations with 3 or more, 2 or more, and 1 or more plants within 5 km, respectively. Columns (4)–(5) present results for stations with no nearby plants. Columns (1)–(4) include weather controls, city by year fixed effects, station by year fixed effects, and year-month fixed effects. Column (5) replaces year-month FE with province by year-month fixed effects. Standard errors are reported in parentheses and are clustered at the city level. *, **, and *** denote significance at the 10%, 5%, and 1% levels, respectively.

Table A.7: Electric Vehicle Adoption and Other Vehicle Categories

	(1) EV Hybrid	(2) FV
EV hybrid penetration	-2.0095***	
	(0.2241)	
FV penetration		-0.0914***
		(0.0189)
Wind speed	-0.1376	-0.2053
	(4.4009)	(4.4111)
Pressure	0.2257	0.2336
	(0.6723)	(0.6737)
Temperature	-0.0005	-0.0005
	(0.0009)	(0.0009)
Humidity	-0.0293	-0.0292
	(0.0307)	(0.0307)
Constant	4.2444***	4.3074***
	(0.1814)	(0.1837)
Plant FE	Yes	Yes
Year-month FE	Yes	Yes
Observations	250,838	250,838
R^2	0.7600	0.7600

Notes: The table reports fixed-effects regression estimates. All specifications include plant fixed effects and year-month fixed effects. Standard errors are reported in parentheses and are clustered at the city level. *, **, and *** indicate significance at the 10%, 5%, and 1% levels, respectively.

Table A.8: EV Adoption and Air Pollution near Renewable Energy Plants

	(1) NO_2 (10 km)	(2) NO_2 Downwind	(3) NO_2 Upwind
Panel A: Hydropower Plants			
EV penetration	0.1557	0.1338	0.1857
	(0.1556)	(0.1640)	(0.1581)
Observations	48,108	48,019	48,042
R^2	0.7200	0.7141	0.7079
Panel B: Wind Power Plants			
EV penetration	0.5381	0.4593	0.6064
	(0.6572)	(0.6479)	(0.6657)
Observations	357,285	356,548	356,643
R^2	0.7236	0.7231	0.7131
Panel C: Solar Power Plants			
EV penetration	0.3751	0.2993	0.4606
	(0.4924)	(0.4909)	(0.4966)
Observations	358,847	358,268	358,245
R^2	0.7186	0.7176	0.7097
Plant FE	Yes	Yes	Yes
Year-month FE	Yes	Yes	Yes
Weather controls	Yes	Yes	Yes

Notes: This table reports placebo tests examining the relationship between EV penetration and air pollution near renewable energy power plants that do not emit local air pollutants. The dependent variables are NO_2 concentrations measured within 10 km of each plant and along downwind and upwind directions where indicated. Panel A shows results for hydropower plants, Panel B for wind power plants, and Panel C for solar power plants. All specifications include plant fixed effects, year-month fixed effects, and weather controls. Standard errors are reported in parentheses and are clustered at the city level. *, **, and *** denote significance at the 10%, 5%, and 1% levels, respectively.

Table A.9: Effects of EV Adoption on Air Pollution near Retired Power Plants

	(1) $\ln NO_2$	(2) $\ln SO_2$	(3) $\ln PM_{2.5}$
EV penetration	0.0655	-0.0929	-0.0256
	(0.0503)	(0.2121)	(0.0259)
Wind speed	-0.0581***	-0.1016***	-0.0320***
	(0.0077)	(0.0174)	(0.0032)
Pressure	0.0159***	-0.0133**	-0.0010
	(0.0030)	(0.0064)	(0.0008)
Temperature	-0.0126***	-0.0641***	0.0029***
	(0.0029)	(0.0078)	(0.0110)
Humidity	-0.0055***	-0.0016	0.0025***
	(0.0005)	(0.0016)	(0.0002)
Constant	-9.3521***	34.6068***	0.5206
	(3.2452)	(7.2896)	(0.7352)
Plant FE	Yes	Yes	Yes
Year–month FE	Yes	Yes	Yes
Observations	47,056	42,842	46,853
R^2	0.9072	0.6838	0.6993

Notes: This table reports placebo tests examining the relationship between EV penetration and air pollution near retired power plants. The dependent variables are the natural logarithms of NO_2, SO_2, and $PM_{2.5}$ concentrations measured near each retired plant during 2019-2022. All specifications include plant fixed effects and year-month fixed effects, as well as weather controls. Standard errors are reported in parentheses and are clustered at the city level. *, **, and *** denote significance at the 10%, 5%, and 1% levels, respectively.

Table A.10: Definition of Geographical Regions and Included Provinces

Region	**Included Provinces**
North China	Beijing, Tianjin, Hebei, Shanxi, Inner Mongolia
Northeast	Liaoning, Jilin, Heilongjiang
East China	Shanghai, Jiangsu, Zhejiang, Anhui, Fujian, Jiangxi, Shandong
Central China	Henan, Hubei, Hunan
South China	Guangdong, Guangxi, Hainan
Northwest	Shaanxi, Gansu, Qinghai, Ningxia, Xinjiang
Southwest	Chongqing, Sichuan, Guizhou, Yunnan, Tibet

Note: This classification is based on standard geographical and power-grid divisions used in Chinese statistical reporting.

Table A.11: Back-of-the-Envelope Cost–Benefit Analysis of EV Adoption: VLBW Evidence

Channel	Estimate (USD)	Source/Adjustment
(1) Cost due to **infant death**	\$236,900	
Change in infant mortality per VLBW ×	0.206	Matthews et al. (2015)
Cost of infant mortality (VSL)	\$1,150,000	Fan et al. (2020)
(2) **Infant medical care cost**	\$14,867	CHNN (2022)
(3) **Childhood disability cost**	\$16,354	
Change in neurosensory disability per VLBW ×	0.11	Hack et al. (2002)
Cost of childhood disability (18 years)	\$148,672	WHO/World Bank
(4) **Cost due to reduction in adult income**	\$18,152	
Average lifetime income	\$550,050	NBS China (2022)
Percent income loss from VLBW	0.033	Bharadwaj et al. (2018)
(5) **Cost of adult disability (medical care)**	\$14,867	
Change in adult disability per VLBW ×	0.1	Hack et al. (2002)
Cost of adult disability medical care (ages 19–67)	\$148,672	Anderson et al. (2010) Adjusted
(6) **Cost of long-term mortality risk**	\$280,891	
Average change in life expectancy ×	11.6 years	Bharadwaj et al. (2018)
Statistical value of year of life	\$24,215	Huang et al. (2017) Adjusted
Total Social Cost per VLBW Birth	**\$582,031**	
Aggregate Health Benefits (Main Analysis)		
Annual Savings: 5,229 avoided VLBW births	**\$3.04 billion**	Urban Estimates
Cumulative Savings (2019–2022)	**\$12.17 billion**	
Distributional Burden of Pollution Displacement		
Annual Additional Cost: 372 induced VLBW births	**\$0.22 billion**	Power Plant Estimates
Cumulative Burden (2019–2022)	**\$0.87 billion**	

Notes: This table presents the calculation of social costs per very low birth weight (VLBW, defined as birth weight $<$ 1,500 grams) infant and the aggregate welfare implications of electric vehicle adoption. The table decomposes the total social cost into six channels: infant mortality, medical care, childhood disability, adult income loss, adult disability, and long-term mortality risk, following the framework of Matthews et al. (2015) and Cutler and Meara (2000). All cost estimates are calibrated to 2022 USD using China-specific parameters and the 2022 average exchange rate (6.73 CNY/USD). Population and VLBW incidence data are from the National Bureau of Statistics (2019–2022) and the Chinese Neonatal Network (CHNN). Based on an average annual birth population of 11.708 million and a 0.7 percent VLBW incidence rate, the baseline is 81,956 VLBW infants annually. Aggregate health benefits are estimated using ground-level monitoring data from the *China City Statistical Yearbook*. Distributional burdens are estimated using satellite-derived pollution concentrations near power plants. Due to data source heterogeneity, the urban and power plant estimates are not numerically comparable and should not be directly summed or netted out.

B Wind-Adjustment Pollution

Let $\theta_{it}^{\text{wind}}$ be the wind direction angle for plant i in month t, calculated as atan $2\,(v_{it}, u_{it})$. Let ϕ_{ij} be the bearing angle of pixel j relative to plant i. We define the set of downwind pixels $\Omega_{it}^{\text{down}}$ as:

$$\Omega_{it}^{\text{down}} = \left\{ j \,\middle|\, \min\left(\left| \phi_{ij} - \theta_{it}^{\text{wind}} \right|, 2\pi - \left| \phi_{ij} - \theta_{it}^{\text{wind}} \right| \right) \leq \frac{\pi}{4} \right\}. \tag{A.1}$$

The aggregated pollution for the downwind zone at distance d is:

$$Y_{idt}^{\text{down}} = \frac{1}{N_{idt}} \sum_{j \in \left(\Omega_{it}^{\text{down}\ n} \cap \text{Dist}_{\ d} \right)} P_{jt}. \tag{A.2}$$

C Unit Conversion of Air Pollution Measures

Pollution data from Sentinel-5P (TROPOMI) are originally reported as vertical column densities, measured in moles per square meter (mol/m^2). To improve interpretability and facilitate comparison with regulatory standards and prior studies, we convert these column measures into near-surface mass concentrations.

Let $\tilde{P}_{igt}$ denote the satellite-retrieved vertical column density of pollutant P for grid i in month t, measured in mol/m^2. We convert this measure into a volumetric concentration P_{igt} in μg/m^3 using the following transformation:

$$P_{igt} = \tilde{P}_{igt} \times \frac{MW_P \times 10^6}{H}, \tag{A.3}$$

where MW_P denotes the molecular weight of pollutant P (in g/mol), H is the assumed effective atmospheric mixing height (in meters), and 10^6 converts grams to micrograms.

Following the applied literature, we assume a uniform planetary boundary layer height of $H = 1{,}000$ meters. This assumption affects the level of the converted concentration but does not affect relative spatial or temporal variation, which is the primary source of identification in our empirical strategy. Table C.1 summarizes the molecular weights used in the conversion and the resulting units.

The conversion involves only constant multiplicative factors for each pollutant and therefore preserves all relative variation across space and time. As a result, coefficient signs, statistical significance, and goodness-of-fit are invariant to the conversion. All empirical results reported in the main text use pollution measures expressed in μg/m^3.

This approach is standard in studies combining satellite-derived pollution measures with

Table C.1: Conversion of Air Pollution Measures to $\mu g/m^3$

Pollutant	Original Unit	Molecular Weight (g/mol)	Final Unit
NO_2	mol/m^2	46.01	$\mu g/m^3$
SO_2	mol/m^2	64.07	$\mu g/m^3$
O_3	mol/m^2	48.00	$\mu g/m^3$

Notes: Satellite-based pollution measures are originally reported as vertical column densities in mol/m^2. We convert these measures into near-surface mass concentrations using standard molecular-weight transformations and an assumed uniform planetary boundary layer height. This conversion affects levels but preserves all relative spatial and temporal variation used for identification.

ground-level economic outcomes and ensures consistency with regulatory benchmarks and prior empirical work.

D Conceptual Model of Pollution Redistribution

This appendix presents a simple conceptual framework that clarifies how electric vehicle (EV) adoption can simultaneously improve air quality in urban areas while worsening pollution exposure in communities located near fossil-fuel power plants. The model formalizes conditions under which EV adoption increases environmental inequality both within and across cities, consistent with the empirical findings in the paper.

D.1 Environment

Consider an economy with two locations: (i) the **city** (C), where households live and adopt EVs, and (ii) the **plant community** (P), where a coal-fired power plant is located. Let $s \in [0, 1]$ denote the share of vehicles in the city that are electric. Time is static, and the total number of vehicles is normalized to one.

D.2 Emissions

There are two sources of pollution: (i) tailpipe emissions from gasoline vehicles and (ii) power-plant emissions from electricity used to charge EVs.

Tailpipe emissions. Each gasoline vehicle emits $e_T > 0$ units of local pollution. Thus,

$$E_T^C(s) = (1 - s)e_T. \tag{A.4}$$

Power-plant emissions. Each EV consumes $k_E > 0$ units of electricity. Total electricity demand is therefore

$$Q(s) = k_E s. \tag{A.5}$$

The coal plant emits $e_P > 0$ units of pollution per unit of electricity, yielding

$$E_P(s) = e_P k_E s. \tag{A.6}$$

D.3 Pollution Transport and Damages

A fraction $\lambda_C \in [0, 1)$ of power-plant emissions drift back toward the city, while a larger fraction $\lambda_P \in (0, 1]$ affects the plant community, with $\lambda_P \gg \lambda_C$. Exposure levels are:

$$X_C(s) = E_T^C(s) + \lambda_C E_P(s), \quad X_P(s) = \lambda_P E_P(s). \tag{A.7}$$

Let $d_C, d_P > 0$ denote marginal damages per unit exposure. Damages are therefore:

$$D_C(s) = d_C X_C(s), \quad D_P(s) = d_P X_P(s). \tag{A.8}$$

D.4 Benefits of EV Adoption

Households in the city receive private benefits from EV adoption, such as fuel savings and reduced local pollution. Let $b > 0$ denote the per-EV private benefit:

$$B_C(s) = bs. \tag{A.9}$$

The plant community receives no direct benefit: $B_P(s) = 0$.

D.5 Welfare

Welfare in each location is defined as

$$W_C(s) = B_C(s) - D_C(s), \quad W_P(s) = -D_P(s). \tag{A.10}$$

D.6 Distributional Effects of EV Adoption

We characterize who gains and who loses from a marginal increase in EV adoption.

D.6.1 City welfare

Differentiating,

$$\frac{dW_C}{ds} = b + d_C e_T - d_C \lambda_C e_p k_E \tag{A.11}$$

Proposition 1. *EV adoption increases welfare in the city if and only if*

$$b + d_C e_T > d_C \lambda_C e_P k_E \tag{A.12}$$

City residents gain from (i) private EV benefits b and (ii) reduced tailpipe emissions $d_C e_T$, but lose from the small fraction of power-plant emissions that drift back toward the city.

D.6.2 Plant-community welfare

Differentiating,

$$\frac{dW_P}{ds} = -d_P \lambda_P e_P k_E < 0. \tag{A.13}$$

Proposition 2. *Communities near power plants always experience lower welfare from higher EV adoption unless the electricity grid is fully decarbonized ($e_P = 0$).*

Because plant communities bear most of the upstream emissions (λ_P large), they are harmed by increased electricity demand induced by EVs.

D.6.3 Environmental inequality

Proposition 3 (Regressive Green Transition)**.** *EV adoption increases environmental inequality when*

$$\frac{dW_C}{ds} > 0 \quad \textit{and} \quad \frac{dW_P}{ds} < 0, \tag{A.14}$$

which holds whenever condition (A.12) is satisfied.

Consumers in the city benefit from EV adoption, while plant-adjacent communities experience higher pollution and lower welfare. This reproduces the within-city environmental inequality documented empirically.

D.7 Extension: Many Cities and Shared Power Plants

Generalize the economy to cities $c = 1, \ldots, C$ and power plants $j = 1, \ldots, J$. Let s_c: EV share in city c, θ_{jc}: share of city c's electricity supplied by plant j, with $\sum_j \theta_{jc} = 1$,

$Q_c(s_c) = k_E s_c$: electricity for EVs, $\psi_{\ell j}$: fraction of plant j's emissions transported to location ℓ, determined by distance and wind direction.

Total emissions from plant j:

$$E_j = e_P \sum_c \theta_{jc} Q_c\left(s_c\right). \tag{A.15}$$

Exposure in any location ℓ:

$$X_\ell = \sum_j \psi_{\ell j} E_j. \tag{A.16}$$

Proposition 4 (Cross-City Inequality)**.** *EV adoption in one city can increase pollution in other cities or rural communities if* $\psi_{\ell j} > 0$ *and* $\theta_{jc} > 0$ *for some* j*.*

Cities that adopt EVs may not be the same locations exposed to the incremental power-plant emissions required to charge those vehicles. This reproduces the *across-city* environmental inequality patterns observed in the data.

The conceptual model clarifies three key insights. First, EV adoption can raise welfare in cities even when electricity generation is polluting. Second, plant communities are harmed by the increase in upstream emissions associated with EV charging. Third, pollution may be redistributed across space in ways that create both within-city and across-city environmental inequality. These theoretical predictions align closely with the empirical results in the paper.

E Electricity Dispatch and Inter-city Transmission

In this section, we provide a high-level summary of the construction of electricity dispatch and transmission lines, which largely follows the algorithm in Arkolakis and Walsh (2023). They provide much greater detail in their replication guide.

E.1 Method

We use Arkolakis and Walsh (2023) algorithm, which takes raw transmission line and power station data and constructs a simplified model of the grid for analysis. Starting from raw OpenStreetMap (OSM) data on power lines, substations, and plants, the grid is abstracted into a simplified network using their multi-step algorithm that clusters nearby stations, cleans line endpoints, splits and merges transmission lines, and removes redundant geometric detail. The output is a set of nodes (stations) and links (transmission lines) with estimated line capacities in megawatts.

We model short-run electricity dispatch as occurring through the existing transmission network, subject to capacity constraints. We do not solve a full unit-commitment or bidding model. Instead, we assume that marginal changes in electricity demand are met by marginal generation capacity available within the connected network.

The method uses a fit of the St. Clair curve as per Gutman et al. (1979) to estimate line capacity using voltage and distance. It relates the distance of a power line to a standardized unit of capacity, which is independent of the line voltage. We can then use the voltage information of each line to back out values of capacity in the more familiar megawatt units.

Line capacities are estimated by first cleaning voltage information from OpenStreetMap (OSM), destringing merged lists, correcting unit inconsistencies (values below 1000 are treated as kilovolts, and values above as volts), and imputing missing voltages using mean values within 25 distance-based bins. We then apply a nonparametric fit of the St. Clair curve from Gutman et al. (1979) to map line distance to transmission capacity. The standardized unit u_i is calculated as:

$$u_i = 0.1021681 + \frac{11.43091 - 0.1021681}{1 + \left(\frac{d_i}{12.49187}\right)^{0.7700907}}, \tag{A.17}$$

where d_i is the distance in miles. Capacity c_i (MW) is then $c_i = \frac{V_i^2}{z} \times u_i$, with surge impedance $z \approx 400$ ohms and voltage V_i in kV. This step adds mean voltages and capacities to the abstracted lines, enabling flow simulations.

We aggregate transmission lines and generation assets to the prefecture–city level. Power plants from the Global Power Plant Database are spatially intersected with city boundaries

and summed by city, with capacities decomposed into renewable and non-renewable components. For transmission lines, endpoints are assigned to cities, and voltages, capacities, line counts, and distances are aggregated for each city pair to form representative edges connecting city centroids. This procedure yields adjacency matrices capturing connectivity, transmission capacity, voltage, and distance, consistent with China's regional grid structure.

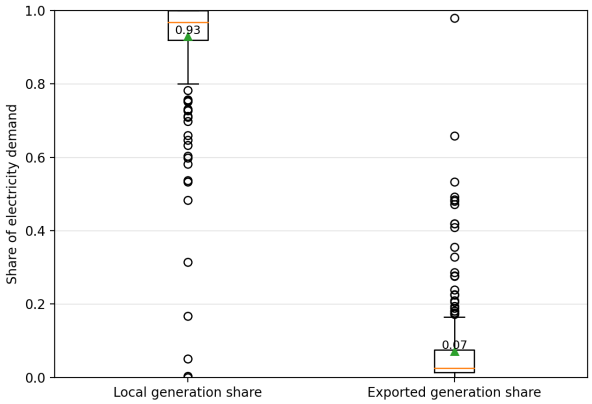
This aggregation produces a city-by-city transmission network summarized by an adjacency matrix of intercity connections, with entries capturing total transmission capacity between each pair of cities.

E.2 Power Grid Transmission in China

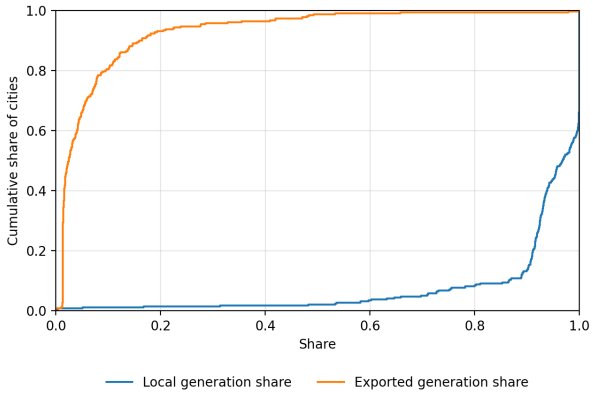
Figure E.1 illustrates how electricity demand induced by electric vehicle adoption is met through local generation and intercity transmission. Panel (a) shows that, for most cities, the majority of electricity demand is supplied by local generation, reflecting the importance of within-city capacity in meeting short-run demand. At the same time, a nontrivial share of electricity demand is supplied by generation in other cities through the transmission network. Panel (b) highlights the heterogeneity in this pattern across cities: while many cities rely almost exclusively on local generation, a meaningful subset exhibits substantial reliance on intercity electricity dispatch. This spatial reallocation of electricity generation provides a key channel through which EV adoption can shift pollution exposure across locations rather than uniformly reducing it.[21]

Figure E.2 visualizes the intercity allocation of electricity generation serving major urban demand centers. The flows show how electricity demand in Beijing, Shanghai, Guangzhou, and Shenzhen is met by generation from multiple cities through the transmission network. For each destination city, incoming flows are normalized to sum to one, highlighting the relative contribution of different generation locations rather than absolute quantities. While local and nearby generation accounts for a substantial share of electricity supply, a meaningful fraction is provided by more distant cities, underscoring the importance of intercity transmission. This spatial reallocation of electricity generation provides a mechanism through which changes in urban electricity demand can shift associated emissions across locations.

[21] We are happy to share the data describing the electricity transmission across cities in China.



(a) Local vs. exported electricity generation



(b) Distribution of shares across cities

Figure E.1: Electricity dispatch induced by electric vehicle adoption

Notes: Panel (a) shows the distribution of the share of electricity demand served by local generation versus generation in other cities. Panel (b) plots the cumulative distribution functions of local and exported generation shares across cities. Electricity dispatch is constructed using the transmission network following Arkolakis and Walsh (2023). Exported generation reflects electricity supplied through intercity transmission links rather than local generation.

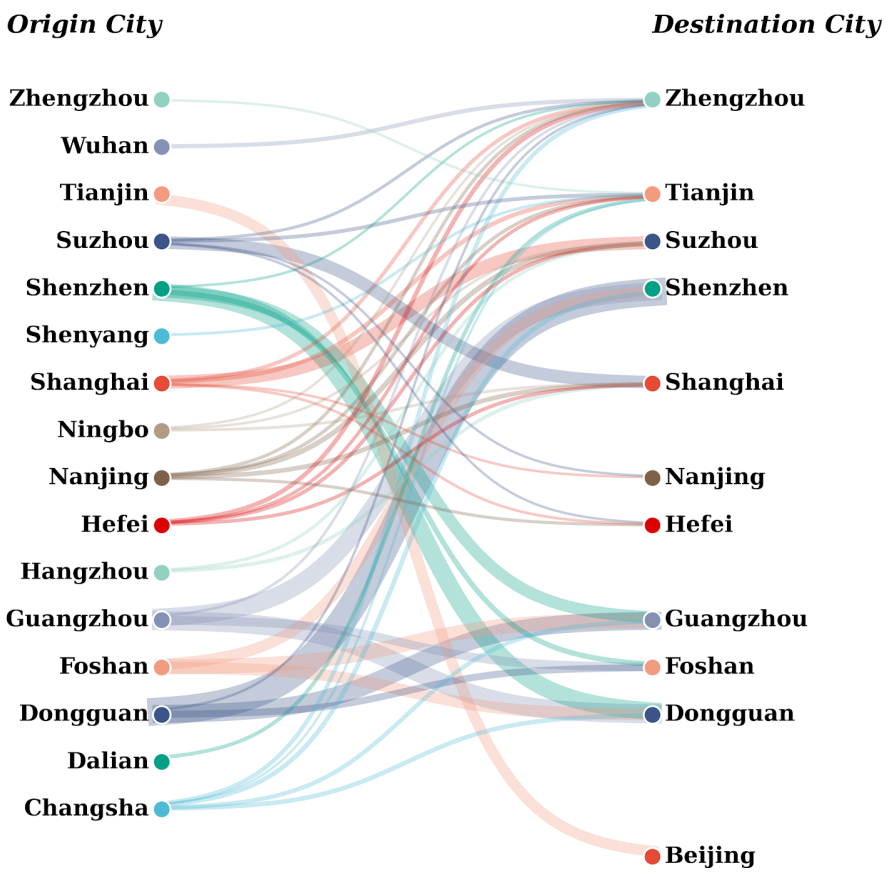


Figure E.2: Electricity dispatch across cities

Notes: This figure illustrates the inter-city electricity dispatch flows between major Chinese urban centers. The left axis represents the originating cities (producers/exporters), and the right axis represents the destination cities (consumers/importers). The width of the connecting bands is proportional to the volume of electricity dispatched.